
Distribution-Aligned Decoding for Efficient LLM Task Adaptation

Senkang Hu^{1,2,*}, Xudong Han^{3,*}, Jinqi Jiang⁴, Yihang Tao^{1,2}, Zihan Fang^{1,2}
 Yong Dai⁵, Sam Tak Wu Kwong⁶, Yuguang Fang^{1,2,†}

¹Hong Kong JC STEM Lab of Smart City, ²City University of Hong Kong, ³University of Sussex,

⁴Huazhong University of Science and Technology, ⁵Fudan University, ⁶Lingnan University

{senkang.forest, yihang.tommy, zihanfang3-c}@my.cityu.edu.hk,
 xh218@sussex.ac.uk, jinqijiang667@gmail.com, daiyongya@outlook.com,
 samkwong@ln.edu.hk, my.Fang@cityu.edu.hk

Abstract

Adapting billion-parameter language models to a downstream task is still costly, even with parameter-efficient fine-tuning (PEFT). We re-cast task adaptation as output-distribution alignment: the objective is to steer the output distribution toward the task distribution directly during decoding rather than indirectly through weight updates. Building on this view, we introduce Steering Vector Decoding (SVD), a lightweight, PEFT-compatible, and theoretically grounded method. We start with a short warm-start fine-tune and extract a task-aware steering vector from the Kullback-Leibler (KL) divergence gradient between the output distribution of the warm-started and pre-trained models. This steering vector is then used to guide the decoding process to steer the model’s output distribution towards the task distribution. We theoretically prove that SVD is first-order equivalent to the gradient step of full fine-tuning and derive a globally optimal solution for the strength of the steering vector. Across three tasks and nine benchmarks, SVD paired with four standard PEFT methods improves multiple-choice accuracy by up to 5 points and open-ended truthfulness by 2 points, with similar gains (1-2 points) on commonsense datasets without adding trainable parameters beyond the PEFT adapter. SVD thus offers a lightweight, theoretically grounded path to stronger task adaptation for large language models.

1 Introduction

Large language models (LLMs) [1, 2, 3, 4] are pivotal in AI, marking early steps towards artificial general intelligence (AGI). They excel in tasks like language understanding, generation, and translation, transforming natural language processing with their grasp of context and human intent. Models like DeepSeek-R1 [4] and OpenAI o1 [5] demonstrate strong reasoning and multimodal capabilities, respectively. Specialized models such as EmoLLMs [6], LMDrive [7], and AnomalyGPT [8] address specific downstream tasks like affective instructions, autonomous driving, and anomaly detection. Despite their capabilities, LLMs are resource-intensive, often requiring hundreds of millions to billions of parameters. For instance, training a LLaMA-7B model demands at least 58 GB of memory [9], which is beyond the capacity of consumer-grade hardware like the NVIDIA RTX 4090 with 24GB, limiting their broader applications.

To tackle this challenge, parameter-efficient fine-tuning (PEFT) [10, 11, 12, 13, 14, 15] has emerged as a key area of progress in modifying LLMs with minimal computational and GPU memory demands.

*Equal contribution

†Corresponding author

This approach focuses on updating a few trainable parameters to significantly reduce the memory footprint while enhancing the performance on downstream tasks. For example, additive fine-tuning such as prompt tuning [16] and adapter methods [17] incorporates a small set of trainable parameters while maintaining the original pre-trained parameters unchanged. Selective fine-tuning such as Diff Pruning [18] chooses a subset of the model’s existing parameters to undergo updates during training. Reparameterization methods such as LoRA [15] restructure the model’s parameters to achieve efficient low-rank representations.

However, while PEFT methods effectively reduce the cost of training adaptation, the adaptation process itself is still primarily viewed through the lens of modifying model weights to change the model’s output distribution to match the task-specific target distribution, which requires backward passes, optimizing states, and multiple training epochs.

Why do We Still Chase the Weights? The end goal of adaptation is not to adjust internal tensors. It is to *shift the model’s output distribution* so that $P_\theta(y|x)$ aligns with the task-specific target. Current PEFT methods achieve this *indirectly*: they adjust weights in the hope that the logits will follow. However, this indirect approach leads to three practical issues: 1) training still scales linearly in model size and data epochs; 2) weight updates can have unpredictable, non-local effects on token probabilities; and 3) a fixed PEFT hyper-parameter often fails to transfer across tasks and domains.

A Distribution-First Perspective. To answer this question, we propose a shift in perspective, rethinking task adaptation not just as a weight-update problem but fundamentally as a process of aligning the model’s output distribution with the task-specific target distribution. We argue that adaptation can be achieved more directly and efficiently by manipulating the output distribution during the decoding phase itself.

Steering Vector Decoding (SVD). To achieve this goal, we present Steering Vector Decoding (SVD), an innovative, efficient, and PEFT-compatible method for task adaptation. SVD begins with a short *warm-start* fine-tuning phase to obtain the warm-started model, whose output distribution is closer to the task-specific target compared to the pre-trained model. Then we can capture the task-specific direction from the differences between output distributions of the warm-started model and the pre-trained model. Specifically, we first compute the KL divergence between these two distributions, and then use the negative gradient of the KL divergence to construct the steering signal. Next, this signal is mapped from the distribution space to the logit space to avoid simplex geometry violation and yields a task-aware steering vector that tells us which tokens need more (or less) probability mass and by how much. Additionally, confidence-aware constraints are applied to the steering vector to ensure its robustness and stability. Finally, the steering vector is used to adjust the model’s logits at each step during decoding, effectively steering the generation process towards the desired task behavior. Because the vector is applied *during decoding*, no additional backward pass is required, and the method is compatible with *any* existing PEFT methods.

Our contributions are summarized as follows: 1) We rethink LLM task adaptation from the perspective of *output distribution alignment*. 2) We propose the SVD method, which leverages negative gradients of KL divergence between distributions to construct task-aware steering vectors for decoding-time adaptation. 3) We provide theoretical analysis, linking SVD to traditional PEFT methods and derive an analytical solution for the optimal steering strength. 4) We demonstrate through extensive experiments on various tasks and models that SVD, when combined with standard PEFT techniques, consistently improves performance while maintaining computational efficiency.

2 Rethinking LLM Task Adaptation from the Perspective of Output Distribution Alignment

Large language models (LLMs) define a conditional output distribution over tokens or task labels, parameterized by θ , as $P_\theta(y|x) = \text{Softmax}(f_\theta(x))$, where $y = f_\theta(x)$ is the logits vector produced by the model for input x . Fine-tuning adapts the model to a downstream task by updating θ such that the model’s output distribution better aligns with the task-specific target distribution. Specifically, given a downstream dataset $\mathcal{D}_{\text{task}} = \{(x_i, y_i)\}_{i=1}^N$, fine-tuning adjusts θ by minimizing the loss function on the dataset $\mathcal{D}_{\text{task}}$. The standard fine-tuning objective is the negative log-likelihood (NLL):

$$\mathcal{L}_{\text{FT}}(\theta) = -\mathbb{E}_{(x,y) \sim \mathcal{D}_{\text{task}}} [\log P_\theta(y|x)]. \tag{1}$$

This is exactly the cross-entropy between the model’s output distribution and the empirical one-hot distribution of the correct tokens. Minimizing this encourages the model to assign higher probability to the correct token at each position. In the special case where each y_i is a single label (e.g. for classification), this formula reduces to $-\log P_\theta(y_i | x_i)$, the usual cross-entropy for a single-label prediction.

Theorem 1. *The NLL objective in Eq. (1) is equivalent to minimizing the expected Kullback-Leibler (KL) divergence between the empirical label distribution $\hat{P}_{\text{task}}(y | x)$ and the model’s output distribution:*

$$\mathcal{L}_{\text{FT}}(\theta) = \mathbb{E}_{x \sim \mathcal{D}} \left[\text{KL} \left(\hat{P}_{\text{task}}(y | x) \parallel P_\theta(y | x) \right) \right], \quad (2)$$

where $\hat{P}_{\text{task}}(y | x)$ is typically a delta function centered on the ground-truth label.

Proof. Let $\hat{P}_{\text{task}}(y | x) = \delta_{y_i}(y)$ be the empirical distribution over labels for input x_i , where $\delta_{y_i}(y) = 1$ if $y = y_i$ and 0 otherwise. The KL divergence between the empirical distribution and the model’s predicted distribution is defined as:

$$\text{KL} \left(\hat{P}_{\text{task}}(y | x) \parallel P_\theta(y | x) \right) = \sum_{y \in \mathcal{Y}} \hat{P}_{\text{task}}(y | x) \log \frac{\hat{P}_{\text{task}}(y | x)}{P_\theta(y | x)}. \quad (3)$$

where $\mathcal{Y} = \{y_1, y_2, \dots, y_{|\mathcal{Y}|}\}$ is the vocabulary set of the model. Since $\hat{P}_{\text{task}}(y | x)$ is a delta function, only the true label $y = y_i$ contributes:

$$\text{KL} \left(\hat{P}_{\text{task}}(y | x_i) \parallel P_\theta(y | x_i) \right) = \log \frac{1}{P_\theta(y_i | x_i)} = -\log P_\theta(y_i | x_i). \quad (4)$$

Taking the expectation over all samples in the dataset yields:

$$\mathbb{E}_{x \sim \mathcal{D}} \left[\text{KL} \left(\hat{P}_{\text{task}}(y | x) \parallel P_\theta(y | x) \right) \right] = \frac{1}{N} \sum_{i=1}^N [-\log P_\theta(y_i | x_i)], \quad (5)$$

which matches the definition of the average negative log-likelihood as in Eq. (1). Hence, the NLL objective is equivalent to minimizing the expected KL divergence between the task label distribution and the model’s output distribution. \square

Distributional Interpretation. From the output distribution perspective, fine-tuning reshapes the model’s belief $P_\theta(y|x)$ over the output space to align more closely with the true task-specific behavior. The output distribution $P_\theta(y|x)$ resides on the probability simplex $\Delta^{|\mathcal{Y}|-1}$ [19], and fine-tuning can be seen as shifting the model’s position on this simplex toward the optimal region defined by the task. Minimizing the KL divergence from the empirical distribution emphasizes increasing the probability mass on the correct label without penalizing overconfidence in incorrect predictions. This yields a learning dynamic that is both efficient and focused.

3 Method

In this section, we will introduce the details of the proposed method. As shown in Fig. 1, the proposed method includes two steps. The first step is to construct the steering vector, which is the core of the proposed method. It includes several steps, warm-start, KL gradient as steering signal, logit-space projection, and confidence-aware steering vector constraint. The second step is task-aware steering vector decoding, which leverages the steering vector to steer the model’s output distribution with the optimal steering strength for different tasks. The detailed algorithm is shown in Algorithm 1.

3.1 Steering Vector Construction

Warm-Start. In order to construct the steering vector, we first need to know the task-specific direction of the steering vector. Specifically, given a pre-trained LLM with the parameter θ , the model defines a conditional probability $P_\theta(y | x)$ over output text y given input x . If $y = (y^1, \dots, y^T)$ is a sequence of T tokens, this typically factorizes autoregressively as: $P_\theta(y | x) = \prod_{t=1}^T P_\theta(y^t | x, y^{<t})$, where $y^{<t}$ denotes the sequence of previous tokens, x is the input tokens. The model’s prediction for

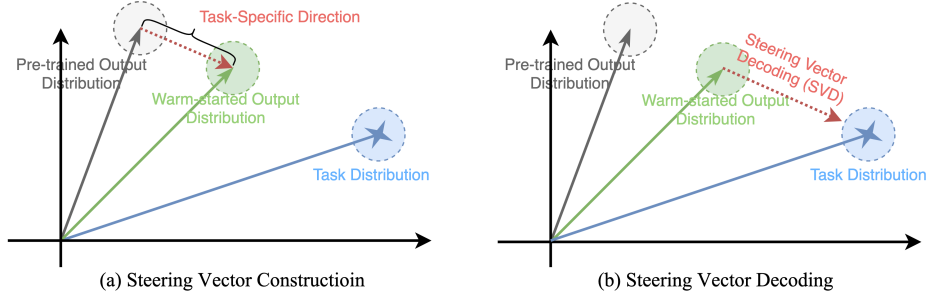


Figure 1: Illustration of the framework of our proposed SVD. It includes two steps: (a) steering vector construction and (b) task-aware steering vector decoding. After the decoding with the steering vector, we can see the warm-started model’s output distribution is steered towards the task-specific target distribution, thereby enhancing the performance of the model on the downstream task.

each token is usually given by a softmax layer producing $P_\theta(y^t | x, y^{<t})$ over the vocabulary at that position.

Given a downstream dataset $\mathcal{D}_{\text{task}} = \{(x_i, y_i)\}_{i=1}^N$, then we warm-start the model by fine-tuning one epoch in $\mathcal{D}_{\text{task}}$ or part of the dataset. This warm-start process can leverage different parameter-efficient fine-tuning strategies, such as additive fine-tuning, selective fine-tuning, and reparametrization fine-tuning discussed in Section A.1.

KL Gradient as Steering Signal. After the warm-start process, the model’s conditional output distribution can be formulated as $P_\phi(y | x)$, where ϕ is the updated parameters, and we believe that the model’s output distribution $P_\phi(y | x)$ is close to the task-specific target distribution $P_{\text{task}}(y | x)$ compared with the pre-trained distribution $P_\theta(y | x)$ since the warm-started model’s training loss decreases and the test accuracy increases.

Then we can leverage the KL divergence to measure the difference between the pre-trained distribution $P_\theta(y | x)$ and the warm-start distribution $P_\phi(y | x)$. Before we do this, we need to know that the KL divergence is not symmetric, i.e., $\text{KL}(M||N) \neq \text{KL}(N||M)$, unless the two distributions are identical (in which case both are 0). If we use $\text{KL}(P_\theta(y | x)||P_\phi(y | x))$ to measure the difference, it means that we assume that the pre-trained model knows more about the task than the warm-started model, and we want to steer the model’s output distribution towards the pre-trained model, which is not what we expect. On the contrary, if we use $\text{KL}(P_\phi(y | x)||P_\theta(y | x))$ to measure the difference, it means that we assume that the warm-started model knows more about the task than the pre-trained model, and we want to steer the model’s output distribution towards the task-specific target distribution. Therefore, we use the following KL divergence to measure the distributional difference:

$$\text{KL}(P_\phi(y | x) || P_\theta(y | x)) = \sum_{y \in \mathcal{Y}} P_\phi(y | x) \log \frac{P_\phi(y | x)}{P_\theta(y | x)} \quad (6)$$

After obtaining the KL divergence, we can use it to construct the steering vector. First, we need to compute the gradient of the KL divergence with respect to $P_\phi(y | x)$, denoted as g_P , which is $\nabla_{P_\phi(y|x)} \text{KL}(P_\phi(y | x) || P_\theta(y | x))$. For clarity, let $P_\phi = P_\phi(y | x)$, $P_\theta = P_\theta(y | x)$. Then $\text{KL}(P_\phi || P_\theta) = \sum_y (P_\phi \log P_\phi - P_\phi \log P_\theta)$. We compute the gradient with respect to P_ϕ (i.e., $\nabla_{P_\phi} \text{KL}$) by taking the partial derivative of KL with respect to each P_ϕ :

$$\frac{\partial \text{KL}}{\partial P_{\phi, y_i}} = \frac{\partial}{\partial P_{\phi, y_i}} (P_{\phi, y_i} \log P_{\phi, y_i} - P_{\phi, y_i} \log P_{\theta, y_i}) = \log \left(\frac{P_{\phi, y_i}}{P_{\theta, y_i}} \right) + 1 \quad (7)$$

Therefore, the gradient $\nabla_{P_\phi} \text{KL}(P_\phi || P_\theta)$ is a vector where each component corresponds to the partial derivative with respect to a specific p_y :

$$\nabla_{P_\phi} \text{KL}(P_\phi || P_\theta) = \left[\log \left(\frac{P_{\phi, y_1}}{P_{\theta, y_1}} \right) + 1, \log \left(\frac{P_{\phi, y_2}}{P_{\theta, y_2}} \right) + 1, \dots, \log \left(\frac{P_{\phi, y_{|\mathcal{Y}|}}}{P_{\theta, y_{|\mathcal{Y}|}}} \right) + 1 \right] \quad (8)$$

The meaning of this gradient is that it indicates how we should adjust P_ϕ to reduce the KL divergence: 1) For a token y_i where $P_{\phi, y_i} > P_{\theta, y_i}$, the gradient component $\log(P_{\phi, y_i}/P_{\theta, y_i}) + 1$ is positive, suggesting we should decrease the probability of this token; 2) For a token y_i where $P_{\phi, y_i} < P_{\theta, y_i}$,

the gradient component is negative, suggesting we should increase the probability of this token. In other words, this gradient points to the direction of returning to the pre-trained distribution P_θ . Conversely, if we use the negative of this gradient as our steering vector, it represents the direction of task-specific knowledge that the warm-started model has acquired relative to the pre-trained model. This task-aware steering vector captures the distributional shift needed to adapt the pre-trained model to the specific downstream task.

Logit-Space Projection. We can leverage the negative gradient of the KL divergence with respect to the output distribution, $-\nabla_{P_\phi} \text{KL}(P_\phi \| P_\theta)$, as a task-aware steering vector. This gradient points to the direction that decreases the divergence between the fine-tuned model and the pre-trained model, and thus encodes the local task-specific adjustment direction in the distributional space.

The simplest approach is to directly apply this vector to adjust the decoding distribution:

$$\hat{P}(y | x) = (1 - \mu) \cdot P_\phi(y | x) + \mu \cdot (-\nabla_{P_\phi} \text{KL}(P_\phi \| P_\theta)) \quad (9)$$

This aims to move P_ϕ closer to the task-optimal distribution P_{task} along the steepest descent direction of KL divergence. However, this method introduces several practical issues: 1) *Normalization Constraint*: Since $P_\phi(y | x)$ is a probability distribution over the vocabulary, the adjusted distribution \hat{P} must satisfy $\sum_y \hat{P}(y | x) = 1$. Directly adding the gradient vector may violate this constraint, requiring techniques such as Lagrangian optimization or projected gradient descent to ensure normalization. 2) *Numerical Stability*: The gradient involves logarithmic terms $\log P_\phi(y)/P_\theta(y)$, which can be numerically unstable when $P_\phi(y)$ or $P_\theta(y)$ are close to zero. To mitigate this, one may apply clipping (e.g., minimum threshold) or smoothing techniques (e.g., adding ϵ) to stabilize the computation. 3) *Simplex Geometry Violation*: The KL gradient is defined in the Euclidean tangent space of the probability simplex. Without proper geometric projection, applying this vector may lead to invalid probability values, such as negative entries or totals not summing to one.

Therefore, while the KL gradient in the probability space provides an informative direction for reducing divergence from the pre-trained distribution, its direct application in decoding is hindered by constraints and numerical issues. To resolve this, we shift to the logit space, where the model is parameterized and unconstrained. By leveraging the chain rule, we can project the KL gradient from probability space into logit space via the softmax Jacobian matrix:

$$\delta_{\text{logits}} = \mathcal{J} \cdot (-\nabla_{P_\phi} \text{KL}(P_\phi \| P_\theta)) = (\text{diag}(P_\phi) - P_\phi P_\phi^\top) \cdot \left(-\log \frac{P_\phi}{P_\theta} - \mathbf{1} \right) \quad (10)$$

This projected vector δ_{logits} serves as a *task-aware logit delta*, which can be added to the original logits before softmax:

$$\hat{z}_\phi = z_\phi + \mu \cdot \delta_{\text{logits}}, \quad \hat{P} = \text{Softmax}(\hat{z}_\phi) \quad (11)$$

This approach preserves the normalization constraint by construction and enables fine-grained control of task-specific adaptation in the model’s output distribution.

Confidence-Aware Steering Vector Constraint. Although the projected task-aware logit delta δ_{logits} captures the KL gradient direction in logit space, it can still be dominated by *false positive tokens*—tokens that are not semantically relevant but receive large KL gradients due to numerical instability (e.g., when $P_\theta(y)$ is extremely small). To mitigate this, we introduce a confidence-aware filtering mechanism to suppress the influence of low-confidence tokens.

We define the confidence of each token $y \in \mathcal{V}$ at a decoding step as its predicted probability under the task-adapted model $s(y) = P_\phi(y | x)$. Let $y^* = \arg \max_{y \in \mathcal{V}} P_\phi(y | x)$ denote the most likely token. Then we introduce a threshold $\alpha \in (0, 1]$ to retain only the confident tokens which have a probability greater than α times the probability of the most likely token. The binary mask $\mathbb{I}(y)$ is defined as:

$$\mathbb{I}(y) = \mathbf{1}(P_\phi(y) \geq \alpha \cdot P_\phi(y^*)) \quad (12)$$

We now mask the logit delta by element-wise applying the confidence mask and penalty:

$$\hat{\delta}_{\text{logits}}(y) = \mathbb{I}(y) \cdot \delta_{\text{logits}}(y) + (1 - \mathbb{I}(y)) \cdot \lambda, \quad (13)$$

where λ is a constant penalty term (e.g., $\lambda = 0, -1$, or a small negative value). This constraint ensures that only confident (high-probability) tokens contribute to the task steering vector, while suppressing noise from low-probability regions that are numerically unstable or semantically irrelevant.

3.2 Task-Aware Steering Vector Decoding

Logit Adjustment. In the decoding process, we first compute the logits $z_\phi(y)$ for each token $y \in \mathcal{V}$ using the task-adapted model $P_\phi(y | x)$. Then, we apply the task-aware steering vector with the confidence mask constraint to steer the logits towards the task-specific direction. The adjusted logits for decoding are then:

$$\hat{z}_\phi(y) = z_\phi(y) + \mu \cdot \hat{\delta}_{\text{logits}}(y) = z_\phi(y) + \mu \cdot (\mathbb{I}(y) \cdot \delta_{\text{logits}}(y) + (1 - \mathbb{I}(y)) \cdot \lambda), \quad (14)$$

where $\mu \in \mathbb{R}$ is a scalar to control the strength of the steering vector. Finally, we apply the softmax function to the adjusted logits to get the adjusted distribution of the output tokens:

$$\hat{P}(y | x) = \text{Softmax}(\hat{z}_\phi(y)) \quad (15)$$

After we get the adjusted distribution, we can leverage different decoding strategies to generate the final output tokens, such as greedy decoding, beam search, and top-k sampling.

Optimal μ as Newton Step. The value of μ is an important hyperparameter that controls the strength of the steering vector. If μ is too small, the steering vector will have little effect on the decoding process. If μ is too large, the steering vector will dominate the decoding process, and the model will be more likely to produce incorrect results. Previous works use fixed μ for all tasks, but here we can derive the optimal μ for each task. Specifically, denoting the distribution of the downstream task as $P_{\text{task}}(y | x)$, we want the distribution of the model’s output as $P_\phi(y | x)$ to be as close as possible to $P_{\text{task}}(y | x)$, that is: finding a μ^* such that the final distribution approximates the task label distribution as closely as possible.

To derive μ^* , we first expand the KL divergence around $\mu = 0$ to obtain the second-order Taylor series:

$$\text{KL}(P_{\text{task}} \| p_\mu) = \text{KL}(P_{\text{task}} \| p_\phi) + \mu \langle \nabla_{z_\phi} \text{KL}(P_{\text{task}} \| p_\phi), \delta_z \rangle + \frac{1}{2} \mu^2 \mathcal{H}[\delta_z] + \mathcal{O}(\mu^3), \quad (16)$$

where $\mathcal{H}[\delta_z] = \delta_z^\top \nabla_{z_\phi}^2 \text{KL}(P_{\text{task}} \| p_\phi) \delta_z$ is the quadratic form of the Hessian. To find the optimal step length μ that minimizes $\text{KL}(P_{\text{task}} \| p_\mu)$, we ignore the constant zeroth-order term and the higher-order terms $\mathcal{O}(\mu^3)$, and consider only the first two orders. Then we take the derivative of these two terms with respect to μ and set it to zero:

$$\frac{d}{d\mu} \left(\mu \cdot \langle \nabla_{z_\phi} \text{KL}(P_{\text{task}} \| p_\phi), \delta_z \rangle + \frac{1}{2} \mu^2 \mathcal{H}[\delta_z] \right) = 0. \quad (17)$$

Solving for μ , we get:

$$\mu^* = - \frac{\langle \nabla_{z_\phi} \text{KL}(P_{\text{task}} \| p_\phi), \delta_z \rangle}{\mathcal{H}[\delta_z]}. \quad (18)$$

which is the exact Newton step. For a one-hot ground-truth label y^* , the task distribution is $P_{\text{task}}(y) = \mathbf{1}_{y=y^*}$, and the gradient of the KL divergence is $\nabla_{z_\phi} \text{KL}(P_{\text{task}} \| p_\phi) = p_\phi - e_{y^*}$, where e_{y^*} is the one-hot basis vector for y^* . Substituting this into the expression for μ^* gives:

$$\mu^* = - \frac{\langle p_\phi - e_{y^*}, \delta_z \rangle}{\mathcal{H}[\delta_z]}. \quad (19)$$

This derivation shows that μ^* is the negative ratio of the linear term to the quadratic term in the Taylor expansion. The exact Newton step requires computing the Hessian $\mathcal{H}[\delta_z]$. However, computing the full Hessian is expensive. We therefore adopt the common Gauss-Newton approximation [20] $\mathcal{H}[\delta_z] \approx \|\delta_z\|_2^2$ (which is exact for a quadratic loss function), yielding

$$\mu^* = \frac{\langle e_{y^*} - p_\phi, \delta_z \rangle}{\|\delta_z\|_2^2 + \epsilon}, \quad (20)$$

where a small ϵ (e.g., 10^{-12}) prevents division by zero when $\|\delta_z\|_2$ is tiny. Finally, we can calculate a global optimal $\bar{\mu}$ by averaging the token-level μ^* over a calibration dataset. The detailed derivation and algorithm can be found in Appendix C and D.

Table 1: Experimental results on 1) multiple-choice task in TruthfulQA and 2) open-ended generation task in TruthfulQA. %T*I stands for %Truth*Info in TruthfulQA.

Model	Method	Multiple-Choice (%)				Open-Ended Generation (%)			
		MC1 ↑	MC2 ↑	MC3 ↑	Avg. ↑	%Truth ↑	%Info ↑	%T*I ↑	Avg. ↑
Qwen2.5-1.5B	Prompt Tuning + SVD	29.88 28.66	43.02 44.47	19.22 21.79	30.71 31.64	28.04 28.66	32.32 33.70	24.39 25.34	28.25 29.23
	IA3 + SVD	40.85 42.19	47.28 55.67	27.51 34.04	38.55 43.97	32.31 34.15	32.93 33.87	28.65 29.87	31.30 32.63
	P-Tuning v2 + SVD	33.54 33.54	45.28 48.41	23.45 25.96	34.09 35.97	31.70 32.32	33.53 32.32	27.44 28.05	30.89 30.90
	LoRA + SVD	50.61 52.94	55.55 61.41	34.81 34.95	46.99 49.77	49.39 50.00	43.90 44.52	40.85 42.68	44.71 45.73
Qwen2.5-7B	Prompt Tuning + SVD	51.95 53.25	49.34 62.16	35.17 35.45	45.49 50.29	64.02 65.24	62.19 62.80	56.10 57.92	60.77 61.99
	IA3 + SVD	47.56 46.07	50.36 57.04	31.89 31.99	43.27 45.03	52.44 54.26	55.48 55.48	48.78 50.00	52.23 53.25
	P-Tuning v2 + SVD	46.95 48.78	50.23 59.35	33.08 35.09	43.42 47.74	62.19 64.63	67.07 67.68	59.14 60.97	62.80 64.43
	LoRA + SVD	49.39 50.61	51.31 58.33	32.82 34.47	44.51 47.80	54.89 55.48	49.39 50.61	46.34 46.95	50.21 51.01
LLaMA3.1-8B	Prompt Tuning + SVD	35.37 29.61	43.11 55.06	22.43 30.64	33.64 38.44	36.58 37.90	32.32 33.54	28.55 28.66	32.48 33.37
	IA3 + SVD	34.76 30.49	45.83 54.73	24.85 31.89	35.15 39.04	43.90 44.51	47.56 46.95	39.63 40.23	43.70 43.90
	P-Tuning v2 + SVD	38.41 31.71	46.14 49.52	25.91 25.97	36.82 35.73	48.17 48.78	48.78 50.12	42.07 43.68	46.34 47.53
	LoRA + SVD	46.34 48.17	49.12 60.17	33.20 35.07	42.89 47.80	51.21 51.82	44.51 45.12	41.63 42.68	45.78 46.54

4 Experiments

4.1 Experimental Setup

Tasks and Datasets. In order to evaluate the performance of our method, we consider three tasks:

1. *Multiple-Choice Tasks.* For multiple-choice and open-ended generation tasks, we evaluate on the TruthfulQA dataset [21], which is a benchmark designed to measure a model’s tendency to generate truthful answers to questions. We consider three metrics in this task: *MC1*, *MC2*, and *MC3*. The detailed definitions of these metrics are shown in Appendix E.3.
2. *Open-Ended Generation Tasks.* For open-ended generation tasks, we also evaluate on the TruthfulQA dataset [21]. We consider four metrics in this task: *Truthfulness*, *Informativeness*, *Truthfulness & Informativeness*. The detailed definitions of these metrics are shown in Appendix E.3.
3. *Commonsense Reasoning Tasks.* For commonsense reasoning tasks, we leverage eight datasets including BoolQ [22], PIQA [23], SIQA [24], HellaSwag [25], WinoGrande [26], ARC-easy [27], ARC-challenge [27] and OBQA [28], and we leverage accuracy as the metric. The implementation details are shown in Appendix E.5.

Base Models and PEFT Methods. We consider four latest pre-trained LLMs: Qwen2.5-1.5B [2], Qwen2.5-7B [2], LLaMA3-8B [1], and LLaMA3.1-8B [1] as the base models. In addition, we leverage four PEFT methods to incorporate our method: LoRA [29], P-Tuning v2 [30], Prompt Tuning [16], and IA3 [31]. We elaborate the implementation details in Appendix E.

4.2 Main Results

Multiple-Choice Tasks. Table 1 shows that our approach consistently outperforms baseline PEFT methods. For Qwen2.5-1.5B, SVD with LoRA improves scores from 46.99% to 49.77%. For Qwen2.5-7B, SVD with Prompt Tuning increases scores from 45.49% to 50.29%. For LLaMA3.1-8B, SVD with LoRA boosts scores from 42.89% to 47.80%. Despite occasional MC1 score drops, MC2

Table 2: Experimental results on commonsense reasoning tasks. We evaluate different PEFT methods and our proposed SVD method on Qwen2.5-7B and LLaMA3.1-8B.

Model	Method	BoolQ	PIQA	SIQA	HellaS.	WinoG.	ARC-e	ARC-c	OBQA	Avg.
Qwen2.5-7B	LoRA	59.12	85.71	68.57	78.10	58.79	91.00	82.57	79.77	75.45
	+ SVD	60.09	86.97	70.13	79.23	59.67	93.33	85.62	81.43	77.06
	IA3	71.23	86.61	75.41	89.05	67.22	88.00	81.60	81.54	80.08
	+ SVD	72.69	87.23	76.72	90.31	68.41	92.67	85.12	82.07	81.90
LLaMA3.1-8B	Prompt Tuning	64.00	86.58	67.54	73.30	60.64	83.28	72.02	68.36	71.97
	+ SVD	65.67	87.21	67.79	75.42	62.35	84.05	72.68	69.67	73.11
	P-Tuning v2	59.65	83.67	69.00	78.66	59.00	92.32	81.65	79.18	75.39
	+ SVD	60.71	84.10	71.36	79.72	59.48	92.60	82.33	81.04	76.42
LLaMA3.1-8B	LoRA	74.18	83.21	79.56	95.00	87.92	91.86	83.67	88.52	85.49
	+ SVD	74.74	84.10	80.31	95.48	88.65	92.45	83.98	89.43	86.14
	IA3	69.84	83.67	68.22	85.33	69.00	87.83	73.90	78.01	76.97
	+ SVD	70.32	84.20	68.75	86.08	69.29	88.10	74.66	78.77	77.52
LLaMA3.1-8B	Prompt Tuning	67.64	80.33	64.67	79.58	62.34	83.57	70.33	74.26	72.84
	+ SVD	68.35	82.00	65.00	80.39	63.07	84.63	71.00	75.41	73.73
	P-Tuning v2	65.33	81.55	66.30	82.42	64.48	87.40	73.56	73.80	74.35
	+ SVD	66.12	82.65	67.54	83.58	65.67	87.68	74.32	75.17	75.34

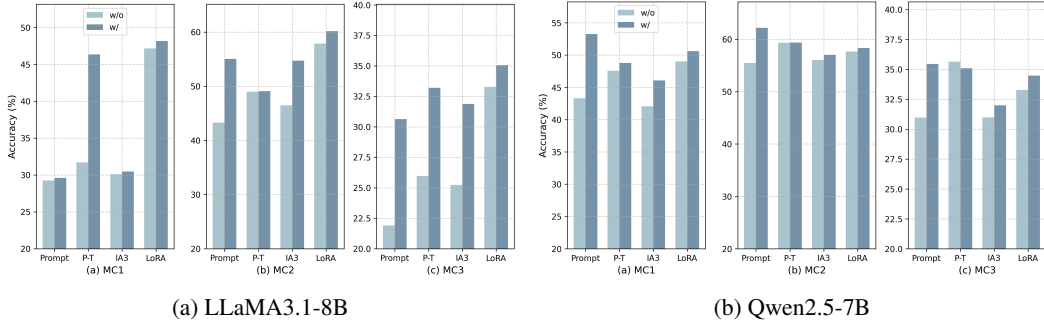


Figure 2: Ablation study on logit-space projection. ‘w/’ means with logit-space projection, ‘w/o’ means without logit-space projection, ‘Prompt’ means Prompt Tuning, and ‘P-T’ means P-Tuning v2. We conduct the ablation study on multiple-choice tasks.

and MC3 improvements ensure overall better performance, highlighting SVD’s effectiveness in enhancing truthful answer selection.

Open-Ended Generation Tasks. Table 1 shows that our approach improves performance across all datasets. For Qwen2.5-1.5B, SVD with LoRA increases the score from 44.71% to 45.73%. For Qwen2.5-7B, SVD with P-Tuning v2 raises the score from 62.80% to 64.43%. For LLaMA3.1-8B, SVD with LoRA boosts the score from 45.78% to 46.54%. This demonstrates SVD’s effectiveness in enhancing model responses.

Commonsense Reasoning Tasks. Table 2 shows that our approach consistently improves the accuracy of all PEFT baselines across multiple commonsense reasoning datasets and models. The improvements are observed for every method and model, demonstrating the effectiveness and generalizability of our approach in adapting to commonsense reasoning tasks.

4.3 Ablation Study

Logit-Space Projection Ablation Study. Figure 2 illustrates the impact of logit-space projection on model performance. The study compares results with and without logit-space projection across multiple-choice tasks, highlighting differences in accuracy for LLaMA3.1-8B and Qwen2.5-7B models. From the figure, we can see that without logit-space projection, the performance of the method drops in all metrics and across all PEFT methods, some of them even drop 10% in accuracy. These

Table 5: Study on the absence of confidence-aware constraint. ‘w/’ means with and ‘w/o’ means without confidence-aware constraint. The PEFT method is LoRA.

Qwen2.5-7B	%Truth	%Info	%T*I
w	55.48	50.61	46.95
w/o	0.02	0.01	0.00

optimal steering strength. In addition, we have proved the equivalence between SVD and the gradient step of fine-tuning, thereby grounding the method in the classical optimization theory. In summary, SVD offers a lightweight, theoretically grounded, and empirically validated path toward stronger LLM task adaptation, bridging the gap between gradient-based fine-tuning and decoding-time control of model behavior, and demonstrating that shifting distributions, not weights, can be the shortest route to better performance.

6 Acknowledgement

The research work described in this paper was conducted in the JC STEM Lab of Smart City funded by The Hong Kong Jockey Club Charities Trust under Contract 2023-0108. The work was supported in part by the Hong Kong SAR Government under the Global STEM Professorship and Research Talent Hub. The work of S. Hu was supported in part by the Hong Kong Innovation and Technology Commission under InnoHK Project CIMDA.

References

- [1] AI@Meta. Llama 3 Model Card. 2024.
- [2] An Yang, Baosong Yang, Binyuan Hui, Bo Zheng, Bowen Yu, Chang Zhou, Chengpeng Li, Chengyuan Li, and et al. Qwen2 Technical Report. *arXiv preprint arXiv:2407.10671*, 2024.
- [3] DeepSeek-AI, Aixin Liu, Bei Feng, Bing Xue, Bingxuan Wang, Bochao Wu, Chengda Lu, Chenggang Zhao, and et al. DeepSeek-V3 Technical Report, 2025. *arXiv preprint arXiv:2412.19437*.
- [4] DeepSeek-AI, Daya Guo, Dejian Yang, Haowei Zhang, and et al. DeepSeek-R1: Incentivizing Reasoning Capability in LLMs via Reinforcement Learning, 2025. *arXiv preprint arXiv:2501.12948*.
- [5] OpenAI, Aaron Jaech, and et al. OpenAI o1 System Card, 2024. *arXiv preprint arXiv:2412.16720*.
- [6] Zhiwei Liu, Kailai Yang, Qianqian Xie, Tianlin Zhang, and Sophia Ananiadou. EmoLLMs: A Series of Emotional Large Language Models and Annotation Tools for Comprehensive Affective Analysis. In *Proceedings of the 30th ACM SIGKDD Conference on Knowledge Discovery and Data Mining, KDD '24*, page 5487–5496, New York, NY, USA, 2024. Association for Computing Machinery. ISBN 9798400704901. doi: 10.1145/3637528.3671552.
- [7] Hao Shao, Yuxuan Hu, Letian Wang, Guanglu Song, Steven L. Waslander, Yu Liu, and Hongsheng Li. LMDrive: Closed-Loop End-to-End Driving with Large Language Models. In *2024 IEEE/CVF Conference on Computer Vision and Pattern Recognition (CVPR)*, pages 15120–15130, 2024. doi: 10.1109/CVPR52733.2024.01432.
- [8] Zhaopeng Gu, Bingke Zhu, Guibo Zhu, Yingying Chen, Ming Tang, and Jinqiao Wang. AnomalyGPT: detecting industrial anomalies using large vision-language models. In *Proceedings of the Thirty-Eighth AAAI Conference on Artificial Intelligence and Thirty-Sixth Conference on Innovative Applications of Artificial Intelligence and Fourteenth Symposium on Educational Advances in Artificial Intelligence, AAAI'24/IAAI'24/EAAI'24*. AAAI Press, 2024. ISBN 978-1-57735-887-9. doi: 10.1609/aaai.v38i3.27963.
- [9] Jiawei Zhao, Zhenyu Zhang, Beidi Chen, Zhangyang Wang, Anima Anandkumar, and Yuandong Tian. GaLore: memory-efficient LLM training by gradient low-rank projection. In *Proceedings of the 41st International Conference on Machine Learning, ICML'24*. JMLR.org, 2024.
- [10] Senkang Hu, Yanan Ma, Yihang Tao, Zhengru Fang, Zihan Fang, Yiqin Deng, Sam Kwong, and Yuguang Fang. Task-Aware Parameter-Efficient Fine-Tuning of Large Pre-Trained Models at the Edge, 2025.
- [11] Zhi Zhang, Qizhe Zhang, Zijun Gao, Renrui Zhang, Ekaterina Shutova, Shiji Zhou, and Shanghang Zhang. Gradient-based Parameter Selection for Efficient Fine-Tuning. In *2024 IEEE/CVF Conference on Computer Vision and Pattern Recognition (CVPR)*, pages 28566–28577, Seattle, WA, USA, June 2024. IEEE. ISBN 979-8-3503-5300-6. doi: 10.1109/CVPR52733.2024.02699.
- [12] Yizhe Xiong, Hui Chen, Tianxiang Hao, Zijia Lin, Jungong Han, Yuesong Zhang, Guoxin Wang, Yongjun Bao, and Guiguang Ding. PYRA: Parallel Yielding Re-activation for Training-Inference Efficient Task Adaptation. In Aleš Leonardis, Elisa Ricci, Stefan Roth, Olga Russakovsky, Torsten Sattler, and Gül Varol, editors, *Computer Vision – ECCV 2024*, volume 15067, pages 455–473. Springer Nature Switzerland, Cham, 2025. ISBN 978-3-031-72672-9 978-3-031-72673-6. doi: 10.1007/978-3-031-72673-6_25. Series Title: Lecture Notes in Computer Science.

- [13] Alan Ansell, Edoardo Ponti, Anna Korhonen, and Ivan Vulić. Composable Sparse Fine-Tuning for Cross-Lingual Transfer. In Smaranda Muresan, Preslav Nakov, and Aline Villavicencio, editors, *Proceedings of the 60th Annual Meeting of the Association for Computational Linguistics (Volume 1: Long Papers)*, pages 1778–1796, Dublin, Ireland, May 2022. Association for Computational Linguistics. doi: 10.18653/v1/2022.acl-long.125.
- [14] Haoyu He, Jianfei Cai, Jing Zhang, Dacheng Tao, and Bohan Zhuang. Sensitivity-Aware Visual Parameter-Efficient Fine-Tuning. In *2023 IEEE/CVF International Conference on Computer Vision (ICCV)*, pages 11791–11801, Paris, France, October 2023. IEEE. ISBN 979-8-3503-0718-4. doi: 10.1109/ICCV51070.2023.01086.
- [15] Edward J Hu, yelong shen, Phillip Wallis, Zeyuan Allen-Zhu, Yuanzhi Li, Shean Wang, Lu Wang, and Weizhu Chen. LoRA: Low-Rank Adaptation of Large Language Models. In *International Conference on Learning Representations, 2022*.
- [16] Brian Lester, Rami Al-Rfou, and Noah Constant. The Power of Scale for Parameter-Efficient Prompt Tuning. In Marie-Francine Moens, Xuanjing Huang, Lucia Specia, and Scott Wen-tau Yih, editors, *Proceedings of the 2021 Conference on Empirical Methods in Natural Language Processing*, pages 3045–3059, Online and Punta Cana, Dominican Republic, November 2021. Association for Computational Linguistics. doi: 10.18653/v1/2021.emnlp-main.243.
- [17] Zhiqiang Hu, Lei Wang, Yihuai Lan, Wanyu Xu, Ee-Peng Lim, Lidong Bing, Xing Xu, Soujanya Poria, and Roy Lee. LLM-Adapters: An Adapter Family for Parameter-Efficient Fine-Tuning of Large Language Models. In Houda Bouamor, Juan Pino, and Kalika Bali, editors, *Proceedings of the 2023 Conference on Empirical Methods in Natural Language Processing*, pages 5254–5276, Singapore, December 2023. Association for Computational Linguistics. doi: 10.18653/v1/2023.emnlp-main.319.
- [18] Demi Guo, Alexander Rush, and Yoon Kim. Parameter-Efficient Transfer Learning with Diff Pruning. In Chengqing Zong, Fei Xia, Wenjie Li, and Roberto Navigli, editors, *Proceedings of the 59th Annual Meeting of the Association for Computational Linguistics and the 11th International Joint Conference on Natural Language Processing (Volume 1: Long Papers)*, pages 4884–4896, Online, August 2021. Association for Computational Linguistics. doi: 10.18653/v1/2021.acl-long.378.
- [19] Karl Heinz Borgwardt. *The simplex method: a probabilistic analysis*, volume 1. Springer Science & Business Media, 2012.
- [20] F. Dan Foresee and M.T. Hagan. Gauss-Newton approximation to Bayesian learning. In *Proceedings of International Conference on Neural Networks (ICNN'97)*, volume 3, pages 1930–1935 vol.3, 1997. doi: 10.1109/ICNN.1997.614194.
- [21] Stephanie Lin, Jacob Hilton, and Owain Evans. TruthfulQA: Measuring how models mimic human falsehoods. In Smaranda Muresan, Preslav Nakov, and Aline Villavicencio, editors, *Proceedings of the 60th Annual Meeting of the Association for Computational Linguistics (Volume 1: Long Papers)*, pages 3214–3252, Dublin, Ireland, May 2022. Association for Computational Linguistics. doi: 10.18653/v1/2022.acl-long.229.
- [22] Christopher Clark, Kenton Lee, Ming-Wei Chang, Tom Kwiatkowski, Michael Collins, and Kristina Toutanova. BoolQ: Exploring the Surprising Difficulty of Natural Yes/No Questions. In Jill Burstein, Christy Doran, and Tamar Solorio, editors, *Proceedings of the 2019 Conference of the North American Chapter of the Association for Computational Linguistics: Human Language Technologies, Volume 1 (Long and Short Papers)*, pages 2924–2936, Minneapolis, Minnesota, 2019. Association for Computational Linguistics. doi: 10.18653/v1/N19-1300.
- [23] Yonatan Bisk, Rowan Zellers, Ronan LeBras, Jianfeng Gao, and Yejin Choi. PIQA: Reasoning about Physical Commonsense in Natural Language. In *The Thirty-Fourth AAAI Conference on Artificial Intelligence, AAAI 2020, The Thirty-Second Innovative Applications of Artificial Intelligence Conference, IAAI 2020, The Tenth AAAI Symposium on Educational Advances in Artificial Intelligence, EAAI 2020, New York, NY, USA, February 7-12, 2020*, pages 7432–7439. AAAI Press, 2020.
- [24] Maarten Sap, Hannah Rashkin, Derek Chen, Ronan Le Bras, and Yejin Choi. Social IQa: Commonsense Reasoning about Social Interactions. In Kentaro Inui, Jing Jiang, Vincent Ng, and Xiaojun Wan, editors, *Proceedings of the 2019 Conference on Empirical Methods in Natural Language Processing and the 9th International Joint Conference on Natural Language Processing (EMNLP-IJCNLP)*, pages 4463–4473, Hong Kong, China, 2019. Association for Computational Linguistics. doi: 10.18653/v1/D19-1454.
- [25] Rowan Zellers, Ari Holtzman, Yonatan Bisk, Ali Farhadi, and Yejin Choi. HellaSwag: Can a Machine Really Finish Your Sentence? In Anna Korhonen, David Traum, and Lluís Màrquez, editors, *Proceedings of the 57th Annual Meeting of the Association for Computational Linguistics*, pages 4791–4800, Florence, Italy, 2019. Association for Computational Linguistics. doi: 10.18653/v1/P19-1472.

- [26] Keisuke Sakaguchi, Ronan Le Bras, Chandra Bhagavatula, and Yejin Choi. WinoGrande: An Adversarial Winograd Schema Challenge at Scale. In *The Thirty-Fourth AAAI Conference on Artificial Intelligence, AAAI 2020, The Thirty-Second Innovative Applications of Artificial Intelligence Conference, IAAI 2020, The Tenth AAAI Symposium on Educational Advances in Artificial Intelligence, EAAI 2020, New York, NY, USA, February 7-12, 2020*, pages 8732–8740. AAAI Press, 2020.
- [27] Peter Clark, Isaac Cowhey, Oren Etzioni, Tushar Khot, Ashish Sabharwal, Carissa Schoenick, and Oyvind Tafjord. Think you have Solved Question Answering? Try ARC, the AI2 Reasoning Challenge, 2018.
- [28] Todor Mihaylov, Peter Clark, Tushar Khot, and Ashish Sabharwal. Can a Suit of Armor Conduct Electricity? A New Dataset for Open Book Question Answering. In Ellen Riloff, David Chiang, Julia Hockenmaier, and Jun’ichi Tsujii, editors, *Proceedings of the 2018 Conference on Empirical Methods in Natural Language Processing*, pages 2381–2391, Brussels, Belgium, 2018. Association for Computational Linguistics. doi: 10.18653/v1/D18-1260.
- [29] Edward Hu, Yelong Shen, Phillip Wallis, Zeyuan Allen-Zhu, Yuanzhi Li, Shean Wang, Lu Wang, and Weizhu Chen. LORA: LOW-RANK ADAPTATION OF LARGE LAN- GUAGE MODELS. 2022.
- [30] Xiao Liu, Kaixuan Ji, Yicheng Fu, Weng Tam, Zhengxiao Du, Zhilin Yang, and Jie Tang. P-Tuning: Prompt Tuning Can Be Comparable to Fine-tuning Across Scales and Tasks. In Smaranda Muresan, Preslav Nakov, and Aline Villavicencio, editors, *Proceedings of the 60th Annual Meeting of the Association for Computational Linguistics (Volume 2: Short Papers)*, pages 61–68, Dublin, Ireland, May 2022. Association for Computational Linguistics. doi: 10.18653/v1/2022.acl-short.8.
- [31] Haokun Liu, Derek Tam, Mohammed Muqeeth, Jay Mohta, Tenghao Huang, Mohit Bansal, and Colin Raffel. Few-shot parameter-efficient fine-tuning is better and cheaper than in-context learning. In *Proceedings of the 36th International Conference on Neural Information Processing Systems, NIPS ’22*, Red Hook, NY, USA, 2022. Curran Associates Inc. ISBN 9781713871088.
- [32] Zeyu Han, Chao Gao, Jinyang Liu, Jeff Zhang, and Sai Qian Zhang. Parameter-Efficient Fine-Tuning for Large Models: A Comprehensive Survey, 2024. arXiv preprint arXiv:2403.14608.
- [33] Neil Houlsby, Andrei Giurgiu, Stanislaw Jastrzebski, Bruna Morrone, Quentin De Laroussilhe, Andrea Gesmundo, Mona Attariyan, and Sylvain Gelly. Parameter-Efficient Transfer Learning for NLP. In Kamalika Chaudhuri and Ruslan Salakhutdinov, editors, *Proceedings of the 36th International Conference on Machine Learning*, volume 97 of *Proceedings of Machine Learning Research*, pages 2790–2799. PMLR, 09–15 Jun 2019.
- [34] Sarkar Snigdha Sarathi Das, Ranran Haoran Zhang, Peng Shi, Wenpeng Yin, and Rui Zhang. Unified Low-Resource Sequence Labeling by Sample-Aware Dynamic Sparse Finetuning. In Houda Bouamor, Juan Pino, and Kalika Bali, editors, *Proceedings of the 2023 Conference on Empirical Methods in Natural Language Processing*, pages 6998–7010, Singapore, December 2023. Association for Computational Linguistics. doi: 10.18653/v1/2023.emnlp-main.433.
- [35] Baohao Liao, Yan Meng, and Christof Monz. Parameter-Efficient Fine-Tuning without Introducing New Latency. In Anna Rogers, Jordan Boyd-Graber, and Naoaki Okazaki, editors, *Proceedings of the 61st Annual Meeting of the Association for Computational Linguistics (Volume 1: Long Papers)*, pages 4242–4260, Toronto, Canada, July 2023. Association for Computational Linguistics. doi: 10.18653/v1/2023.acl-long.233.
- [36] Armen Aghajanyan, Sonal Gupta, and Luke Zettlemoyer. Intrinsic Dimensionality Explains the Effectiveness of Language Model Fine-Tuning. In Chengqing Zong, Fei Xia, Wenjie Li, and Roberto Navigli, editors, *Proceedings of the 59th Annual Meeting of the Association for Computational Linguistics and the 11th International Joint Conference on Natural Language Processing (Volume 1: Long Papers)*, pages 7319–7328, Online, August 2021. Association for Computational Linguistics. doi: 10.18653/v1/2021.acl-long.568.
- [37] Senkang Hu, Zhengru Fang, Yiqin Deng, Xianhao Chen, Yuguang Fang, and Sam Kwong. Toward Full-Scene Domain Generalization in Multi-Agent Collaborative Bird’s Eye View Segmentation for Connected and Autonomous Driving. *IEEE Transactions on Intelligent Transportation Systems*, 26(2):1783–1796, 2025. doi: 10.1109/TITS.2024.3506284.
- [38] Senkang Hu, Yihang Tao, Guowen Xu, Yiqin Deng, Xianhao Chen, Yuguang Fang, and Sam Kwong. CP-Guard: Malicious Agent Detection and Defense in Collaborative Bird’s Eye View Perception. *Proceedings of the AAAI Conference on Artificial Intelligence*, 39(22):23203–23211, Apr. 2025. doi: 10.1609/aaai.v39i22.34486.
- [39] Hao Shao, Yuxuan Hu, Letian Wang, Steven L. Waslander, Yu Liu, and Hongsheng Li. LMDrive: Closed-Loop End-to-End Driving with Large Language Models, 2023.

- [40] Yihang Tao, Senkang Hu, Zhengru Fang, and Yuguang Fang. Directed-CP: Directed Collaborative Perception for Connected and Autonomous Vehicles via Proactive Attention, 2025.
- [41] Senkang Hu, Zhengru Fang, Yiqin Deng, Xianhao Chen, and Yuguang Fang. Collaborative Perception for Connected and Autonomous Driving: Challenges, Possible Solutions and Opportunities. *IEEE Wireless Communications*, pages 1–7, 2025. doi: 10.1109/MWC.002.2400348.
- [42] Senkang Hu, Zhengru Fang, Zihan Fang, Yiqin Deng, Xianhao Chen, Yuguang Fang, and Sam Tak Wu Kwong. AgentsCoMerge: Large Language Model Empowered Collaborative Decision Making for Ramp Merging. *IEEE Transactions on Mobile Computing*, 24(10):9791–9805, 2025. doi: 10.1109/TMC.2025.3564163.
- [43] Qu Yang, Mang Ye, and Bo Du. EmoLLM: Multimodal Emotional Understanding Meets Large Language Models, 2024.
- [44] Senkang Hu, Zhengru Fang, Zihan Fang, Yiqin Deng, Xianhao Chen, and Yuguang Fang. AgentsCoDriver: Large Language Model Empowered Collaborative Driving with Lifelong Learning, 2024.
- [45] Senkang Hu, Yihang Tao, Zihan Fang, Guowen Xu, Yiqin Deng, Sam Kwong, and Yuguang Fang. CP-Guard+: A New Paradigm for Malicious Agent Detection and Defense in Collaborative Perception, 2025.
- [46] Senkang Hu, Yihang Tao, Guowen Xu, Xinyuan Qian, Yiqin Deng, Xianhao Chen, Sam Tak Wu Kwong, and Yuguang Fang. CP-uniGuard: A Unified, Probability-Agnostic, and Adaptive Framework for Malicious Agent Detection and Defense in Multi-Agent Embodied Perception Systems, 2025.
- [47] Zhaopeng Gu, Bingke Zhu, Guibo Zhu, Yingying Chen, Ming Tang, and Jinqiao Wang. AnomalyGPT: Detecting Industrial Anomalies using Large Vision-Language Models. *arXiv preprint arXiv:2308.15366*, 2023.
- [48] Yin Cui, Yang Song, Chen Sun, Andrew Howard, and Serge Belongie. Large Scale Fine-Grained Categorization and Domain-Specific Transfer Learning. In *2018 IEEE/CVF Conference on Computer Vision and Pattern Recognition*, pages 4109–4118, 2018. doi: 10.1109/CVPR.2018.00432.
- [49] Jinsung Yoon, Sercan Arik, and Tomas Pfister. Data Valuation using Reinforcement Learning. In Hal Daumé III and Aarti Singh, editors, *Proceedings of the 37th International Conference on Machine Learning*, volume 119 of *Proceedings of Machine Learning Research*, pages 10842–10851. PMLR, 13–18 Jul 2020.
- [50] Anh Tran, Cuong Nguyen, and Tal Hassner. Transferability and Hardness of Supervised Classification Tasks. In *2019 IEEE/CVF International Conference on Computer Vision (ICCV)*, pages 1395–1405, 2019. doi: 10.1109/ICCV.2019.00148.
- [51] Cuong Nguyen, Tal Hassner, Matthias Seeger, and Cedric Archambeau. LEEP: A New Measure to Evaluate Transferability of Learned Representations. In Hal Daumé III and Aarti Singh, editors, *Proceedings of the 37th International Conference on Machine Learning*, volume 119 of *Proceedings of Machine Learning Research*, pages 7294–7305. PMLR, 13–18 Jul 2020.
- [52] Zihao Fu, Haoran Yang, Anthony Man-Cho So, Wai Lam, Lidong Bing, and Nigel Collier. On the Effectiveness of Parameter-Efficient Fine-Tuning. *Proceedings of the AAAI Conference on Artificial Intelligence*, 37(11):12799–12807, June 2023. ISSN 2374-3468, 2159-5399. doi: 10.1609/aaai.v37i11.26505.
- [53] Ilya Sutskever, Oriol Vinyals, and Quoc V. Le. Sequence to Sequence Learning with Neural Networks. In Z. Ghahramani, M. Welling, C. Cortes, N. Lawrence, and K.Q. Weinberger, editors, *Advances in Neural Information Processing Systems*, volume 27. Curran Associates, Inc., 2014.
- [54] Angela Fan, Mike Lewis, and Yann Dauphin. In Iryna Gurevych and Yusuke Miyao, editors, *Proceedings of the 56th Annual Meeting of the Association for Computational Linguistics (Volume 1: Long Papers)*, pages 889–898, Melbourne, Australia, July 2018. Association for Computational Linguistics. doi: 10.18653/v1/P18-1082.
- [55] Ari Holtzman, Jan Buys, Li Du, Maxwell Forbes, and Yejin Choi. The Curious Case of Neural Text Degeneration. In *8th International Conference on Learning Representations, ICLR 2020, Addis Ababa, Ethiopia, April 26-30, 2020*. OpenReview.net, 2020.

- [56] Xiang Lisa Li, Ari Holtzman, Daniel Fried, Percy Liang, Jason Eisner, Tatsunori Hashimoto, Luke Zettlemoyer, and Mike Lewis. Contrastive Decoding: Open-ended Text Generation as Optimization. In Anna Rogers, Jordan Boyd-Graber, and Naoaki Okazaki, editors, *Proceedings of the 61st Annual Meeting of the Association for Computational Linguistics (Volume 1: Long Papers)*, pages 12286–12312, Toronto, Canada, 2023. Association for Computational Linguistics. doi: 10.18653/v1/2023.acl-long.687.
- [57] Ariel Gera, Roni Friedman, Ofir Arviv, Chulaka Gunasekara, Benjamin Sznajder, Noam Slonim, and Eyal Shnarch. The Benefits of Bad Advice: Autocontrastive Decoding across Model Layers. In Anna Rogers, Jordan Boyd-Graber, and Naoaki Okazaki, editors, *Proceedings of the 61st Annual Meeting of the Association for Computational Linguistics (Volume 1: Long Papers)*, pages 10406–10420, Toronto, Canada, 2023. Association for Computational Linguistics. doi: 10.18653/v1/2023.acl-long.580.
- [58] Yung-Sung Chuang, Yujia Xie, Hongyin Luo, Yoon Kim, James R. Glass, and Pengcheng He. DoLa: Decoding by Contrasting Layers Improves Factuality in Large Language Models. In *The Twelfth International Conference on Learning Representations, ICLR 2024, Vienna, Austria, May 7-11, 2024*. OpenReview.net, 2024.
- [59] Yuxi Xie, Kenji Kawaguchi, Yiran Zhao, James Xu Zhao, Min-Yen Kan, Junxian He, and Michael Qizhe Xie. Self-Evaluation Guided Beam Search for Reasoning. In Alice Oh, Tristan Naumann, Amir Globerson, Kate Saenko, Moritz Hardt, and Sergey Levine, editors, *Advances in Neural Information Processing Systems 36: Annual Conference on Neural Information Processing Systems 2023, NeurIPS 2023, New Orleans, LA, USA, December 10 - 16, 2023*, 2023.
- [60] Cheng-Han Chiang and Hung-yi Lee. Can Large Language Models Be an Alternative to Human Evaluations? In Anna Rogers, Jordan Boyd-Graber, and Naoaki Okazaki, editors, *Proceedings of the 61st Annual Meeting of the Association for Computational Linguistics (Volume 1: Long Papers)*, pages 15607–15631, Toronto, Canada, July 2023. Association for Computational Linguistics. doi: 10.18653/v1/2023.acl-long.870.
- [61] Cheng-Han Chiang and Hung-yi Lee. A Closer Look into Using Large Language Models for Automatic Evaluation. In Houda Bouamor, Juan Pino, and Kalika Bali, editors, *Findings of the Association for Computational Linguistics: EMNLP 2023*, pages 8928–8942, Singapore, December 2023. Association for Computational Linguistics. doi: 10.18653/v1/2023.findings-emnlp.599.
- [62] Xinhao Xu, Hui Chen, Zijia Lin, Jungong Han, Lixing Gong, Guoxin Wang, Yongjun Bao, and Guiguang Ding. TaD: A Plug-and-Play Task-Aware Decoding Method to Better Adapt LLMs on Downstream Tasks. In *Proceedings of the Thirty-Third International Joint Conference on Artificial Intelligence*, pages 6587–6596, Jeju, South Korea, August 2024. International Joint Conferences on Artificial Intelligence Organization. ISBN 978-1-956792-04-1. doi: 10.24963/ijcai.2024/728.

Contents

1	Introduction	1
2	Rethinking LLM Task Adaptation from the Perspective of Output Distribution Alignment	2
3	Method	3
3.1	Steering Vector Construction	3
3.2	Task-Aware Steering Vector Decoding	6
4	Experiments	7
4.1	Experimental Setup	7
4.2	Main Results	7
4.3	Ablation Study	8
5	Conclusion	9
6	Acknowledgement	10
A	Related Work	16
A.1	Parameter-Efficient Fine-Tuning	16
A.2	LLM Task Adaptation	16
A.3	LLM Decoding Strategies	17
B	Mathematical Analysis: Equivalence Between SVD and Fine-Tuning	17
B.1	Notation and Preliminaries	17
B.2	Fine-Tuning Gradient in Logit Space	18
B.3	One SVD Step in Logit Space	19
B.4	First-Order Equivalence Theorem	19
B.5	Conditions for Higher-Order Equivalence	20
C	One-Token Derivation of Optimal Steering Strength μ^*	20
C.1	Setup.	20
C.2	First-Order Taylor Expansion of KL	20
C.3	Optimal Step Length (Newton Approximation)	20
D	One-Token and Dataset-Level Derivation of the Offline Steering Strength $\bar{\mu}$	21
D.1	Per-token optimal strength $\mu_{i,t}^*$	21
D.2	From Tokens to a Global Constant $\bar{\mu}$	21
D.3	Extension to sequences ($T > 1$)	22
E	Experiment Implementation Details	23
E.1	Implementation Details of SVD	23

E.2	Hyperparameters for PEFT Methods	23
E.3	Evaluation Metrics	23
E.4	Implementation Details on Multiple-Choice Tasks and Open-Ended Generation Tasks	26
E.5	Implementation Details on Commonsense Reasoning Tasks	26
E.6	Details about DeepSeek-V3-0324 Evaluation	26
F	More Experiment Results	27
F.1	More Results on Commonsense Reasoning Tasks	27
F.2	Comparison with Other Decoding Adaptation Methods	27
F.3	The Influence of the α Parameter in the Confidence-Aware Constraint.	27
G	Limitations and Future Work	28
H	Practical Impact	28

A Related Work

A.1 Parameter-Efficient Fine-Tuning

As language models continue to increase in scale, traditional full fine-tuning approaches have become increasingly resource-intensive. Parameter-efficient fine-tuning (PEFT) emerges as a practical alternative to address these computational constraints [11, 12, 13, 14, 15]. According to [32], PEFT techniques generally fall into three distinct categories: 1) *Additive Fine-Tuning*, which incorporates a limited set of trainable parameters while maintaining the original pre-trained parameters unchanged. Notable examples in this category include *Adapter* modules [33] and *Prompt Tuning*, which integrates learnable soft prompts into the input. Though effective, these approaches typically introduce additional computational demands during inference. 2) *Selective Fine-Tuning*, which focuses on updating only a carefully chosen subset of the model’s existing parameters [18, 34, 35]. This strategy employs a binary mask \mathcal{M} to selectively determine which parameters undergo updates during training, thereby avoiding the introduction of new parameters. 3) *Reparameterization*, which restructures the model’s parameters to achieve efficient low-rank representations [14, 15, 36]. A prominent example is LoRA [15], which factorizes weight updates into products of smaller matrices, facilitating compact storage of task-specific adaptations. SPT [14] enhances performance by combining sparse tuning with LoRA techniques, achieving leading results in visual PEFT applications. Nevertheless, many existing approaches still lack sufficient task-awareness in their parameter selection mechanisms.

A.2 LLM Task Adaptation

Researchers have developed diverse approaches to adapt pre-trained LLMs for downstream tasks [37, 38, 39, 40, 41, 42, 43, 44, 45, 46, 47] by investigating optimal configurations of pre-training data, model architecture, and weight selection. For instance, Cui *et al.* [48] leverage Earth Mover’s Distance to select the top K most relevant classes from the source domain for task-specific pre-training. Yoon *et al.* [49] apply reinforcement learning techniques to determine appropriate weights for source domain classes. Other approaches assess model transferability to target domains by examining inter-class covariance relationships between source data and target classes, or by analyzing conditional cross-entropy between source and target labels [50, 51]. More recent research focuses on identifying which pre-trained model weights to fine-tune while keeping others frozen [11, 14, 52]. Zhang *et al.* [11] introduced gradient-based parameter selection (GPS), a method that uses gradients to identify optimal tunable weights. Fu *et al.* [52] developed a second-order approximation method (SAM) that approximates the Hessian matrix in the loss function’s second-order Taylor expansion to enhance weight selection precision.

A.3 LLM Decoding Strategies

Decoding methods play a pivotal role in shaping the output characteristics of large language models, determining both the fluency and creativity of generated text. The most basic Greedy Search approach has been observed to frequently fall into repetitive patterns due to its myopic selection strategy. More advanced methods like Beam Search [53] have addressed this limitation by exploring multiple potential sequences simultaneously, though at increased computational cost. Compared to greedy search’s tendency for repetitive outputs and beam search’s limited diversity, Top-k sampling [54] introduces diversity by sampling from a fixed-size set of most probable tokens, while Top-p sampling [55] further improves adaptability by dynamically adjusting the candidate set based on probability mass. Moreover, the introduction of Contrastive Decoding (CD) [56] marks a breakthrough by utilizing comparative analysis between models of different scales to improve generation quality. Building on this foundation, Anticipative Contrastive Decoding (ACD) [57] introduced layer-wise contrastive mechanisms within a single model, while Decoding by Contrasting Layers (DoLa) [58] has advanced the field further through dynamic layer selection algorithms. Guided Decoding (GD) [59] uses the model’s self-evaluation score as a criterion to control the quality of each step and demonstrates higher consistency and robustness in multi-step reasoning. These decoding approaches, however, predominantly emphasize optimizing pre-trained LLM performance without accounting for model transformations that occur during fine-tuning. As a result, they inadequately leverage the task-specific adaptations acquired through fine-tuning processes, which often leads to suboptimal performance gains or even degradation when implemented with fine-tuned LLMs on downstream applications. On the contrary, our method focuses on LLM task adaptation via decoding with task-aware steered vectors, thereby enhancing the performance of LLMs in downstream tasks.

B Mathematical Analysis: Equivalence Between SVD and Fine-Tuning

In this appendix, we prove that a *first-order* Steering-Vector-Decoding (SVD) step is equivalent, in expectation, to one parameter-update step of maximum-likelihood fine-tuning.

B.1 Notation and Preliminaries

Let $z_\theta(x) \in \mathbb{R}^{|V|}$ be the logits produced by the pre-trained LLM for input x and $p_\theta(y | x) = \text{Softmax}(z_\theta(x))$. After a short warm-start fine-tuning, the parameters are ϕ , giving logits z_ϕ and distribution $p_\phi = \text{Softmax}(z_\phi)$.

For a downstream dataset $\mathcal{D}_{\text{task}} = \{(x_i, y_i)\}_{i=1}^N$, the standard fine-tuning objective is the expected negative log-likelihood (NLL):

$$\mathcal{L}_{\text{FT}}(\theta) = -\mathbb{E}_{(x,y) \sim \mathcal{D}_{\text{task}}} [\log p_\theta(y | x)], \quad (21)$$

which is equivalent to $\text{KL}(\hat{p}_{\text{task}} \| p_\theta)$ up to an additive constant, where \hat{p}_{task} is the empirical one-hot distribution.

KL-Gradient Steering Signal. Section 3.1 derives the task-aware direction in probability space as

$$g_P = -\nabla_{p_\phi} \text{KL}(p_\phi \| p_\theta) = -\left[\log\left(\frac{p_\phi}{p_\theta}\right) + \mathbf{1}\right], \quad (22)$$

which is then projected into logit space via the softmax Jacobian:

$$J(p_\phi) = \text{diag}(p_\phi) - p_\phi p_\phi^\top. \quad (23)$$

Thus, the logit-space steering vector is:

$$\delta_z = J(p_\phi) g_P = (\text{diag}(p_\phi) - p_\phi p_\phi^\top) \left[-\log\left(\frac{p_\phi}{p_\theta}\right) - \mathbf{1}\right]. \quad (24)$$

Algorithm 1 Task-Aware Steering Vector for LLM Decoding

Require:

- 1: Pre-trained LLM with parameters θ : $P_\theta(y|x)$.
- 2: Downstream task dataset $\mathcal{D}_{\text{task}} = \{(x_i, y_i)\}_{i=1}^N$.
- 3: Confidence threshold $\alpha \in (0, 1]$ for token filtering.
- 4: Penalty value λ (typically $-\infty$) for low-confidence tokens

Ensure: Task-adapted decoding strategy with steered logits

- 5: **Stage 1: Warm-Start Fine-tuning** ▷ Initialize task-specific parameter distribution
 - 6: Split $\mathcal{D}_{\text{task}}$ into training set $\mathcal{D}_{\text{train}}$ and calibration set $\mathcal{D}_{\text{calib}}$
 - 7: Initialize task-specific parameters $\phi \leftarrow \theta$ ▷ Start from pre-trained parameters
 - 8: Fine-tune model on $\mathcal{D}_{\text{train}}$ to obtain ϕ ▷ Typically 1 epoch is sufficient
 - 9: **function** COMPUTESTEERINGVECTOR(x, P_θ, P_ϕ)
 - 10: Get base model probabilities: $p_\theta \leftarrow P_\theta(\cdot|x)$
 - 11: Get fine-tuned model probabilities: $p_\phi \leftarrow P_\phi(\cdot|x)$
 - 12: **Stage 2: Steering Vector Construction** ▷ Capture task-specific direction
 - 13: Compute KL gradient: $g_P \leftarrow -[\log(p_\phi/p_\theta) + \mathbf{1}]$ ▷ Measure distribution mismatch
 - 14: Compute softmax Jacobian: $J(p_\phi) \leftarrow \text{diag}(p_\phi) - p_\phi p_\phi^\top$
 - 15: Project to logit space: $\delta_z \leftarrow J(p_\phi) \cdot g_P$ ▷ Transform probability gradient to logit space
 - 16: **Stage 3: Apply Confidence-Aware Constraint** ▷ Filter noise and focus on high-confidence tokens
 - 17: Identify most likely token: $y^* \leftarrow \arg \max_{y \in \mathcal{V}} p_\phi(y)$
 - 18: Get threshold probability: $p_{\text{thresh}} \leftarrow \alpha \cdot p_\phi(y^*)$
 - 19: Create confidence mask: $\mathbb{I}(y) \leftarrow \mathbf{1}(p_\phi(y) \geq p_{\text{thresh}})$ ▷ Binary mask for tokens above threshold
 - 20: Apply mask: $\hat{\delta}_z(y) \leftarrow \mathbb{I}(y) \cdot \delta_z(y) + (1 - \mathbb{I}(y)) \cdot \lambda$ ▷ Apply penalty to low-confidence tokens
 - 21: **return** $\hat{\delta}_z$ ▷ Return filtered steering vector
 - 22: **end function**
 - 23: **Stage 4: Calculate Optimal Steering Strength** ▷ Calibrate μ using labeled data
 - 24: Compute global steering constant $\bar{\mu}$ from calibration dataset $\mathcal{D}_{\text{calib}}$ ▷ See Algorithm 2 for details
 - 25: **Stage 5: Decoding with Steering Vector** ▷ Generate task-specific outputs at inference time
 - 26: **function** STEERDECODING($x, P_\phi, P_\theta, \bar{\mu}$)
 - 27: Initialize generated sequence: $y \leftarrow []$
 - 28: **for** each decoding step t until completion **do**
 - 29: Get current context: $x_t \leftarrow (x, y_{<t})$
 - 30: Compute task-adapted logits: $z_{\phi,t} \leftarrow \text{Logits of } P_\phi(\cdot|x_t)$
 - 31: $\hat{\delta}_{z_t} \leftarrow \text{COMPUTE_STEERINGVECTOR}(x_t, P_\theta, P_\phi)$
 - 32: Adjust logits: $\hat{z}_{\phi,t} \leftarrow z_{\phi,t} + \bar{\mu} \cdot \hat{\delta}_{z_t}$ ▷ Apply steering
 - 33: Compute adjusted distribution: $\hat{p}_t \leftarrow \text{Softmax}(\hat{z}_{\phi,t})$
 - 34: Sample/select next token y_t according to chosen decoding strategy
 - 35: Append to sequence: $y \leftarrow [y, y_t]$
 - 36: **end for**
 - 37: **return** y ▷ Complete generated sequence
 - 38: **end function**
 - 39: **return** STEERDECODING function ▷ Return configured decoding function for inference
-

B.2 Fine-Tuning Gradient in Logit Space

For a single training pair (x, y^*) the NLL loss is

$$\begin{aligned}
 \ell(z) &= -\log p(y^* | x) \\
 &= -\log(\text{Softmax}(z_{y^*})) = -\log \frac{e^{z_{y^*}}}{\sum_y e^{z_y}} \\
 &= -z_{y^*} + \log \sum_y e^{z_y}.
 \end{aligned} \tag{25}$$

Its gradient w.r.t. logits is

$$\nabla_z \ell = p - e_{y^*}, \tag{26}$$

where e_{y^*} is the one-hot vector for the correct token. Taking the dataset expectation:

$$\nabla_{z_\phi} \mathcal{L}_{\text{FT}} = \mathbb{E}_{(x, y^*)} [p_\phi - \hat{p}_{\text{task}}]. \quad (27)$$

Because \hat{p}_{task} is one-hot, this is the steepest-descent direction that moves p_ϕ toward the true task distribution.

Derivation of the Gradient To derive $\nabla_z \ell = p - e_{y^*}$, we compute the partial derivative of $\ell(z)$ with respect to each logit z_k :

1. Partial derivative of $-z_{y^*}$: If $k = y^*$, then $\frac{\partial(-z_{y^*})}{\partial z_k} = -1$. If $k \neq y^*$, then $\frac{\partial(-z_{y^*})}{\partial z_k} = 0$. This can be written as $-[e_{y^*}]_k$, where $[e_{y^*}]_k$ is the k -th component of the one-hot vector e_{y^*} .
2. Partial derivative of $\log \sum_y e^{z_y}$: The derivative is $\frac{e^{z_k}}{\sum_y e^{z_y}} = p_k$, where $p = \text{Softmax}(z)$.

Combining these, the partial derivative is:

$$\frac{\partial \ell(z)}{\partial z_k} = p_k - [e_{y^*}]_k. \quad (28)$$

Thus, the gradient vector is given by Eq. 26.

B.3 One SVD Step in Logit Space

SVD perturbs logits during decoding by

$$\tilde{z} = z_\phi + \mu \cdot \delta_z, \quad \tilde{p} = \text{Softmax}(\tilde{z}), \quad (29)$$

where δ_z is given in Eq. 24 and $\mu \in \mathbb{R}$ is a scalar strength (estimated in Appendix C). Because the perturbation is before the softmax, \tilde{p} is always a valid probability distribution.

B.4 First-Order Equivalence Theorem

Theorem 2. Let x be fixed and let $p_\phi(\cdot | x)$ be the warm-started distribution. For any label distribution $q(\cdot)$ and any strength μ , denote the KL divergence after one SVD step by

$$\mathcal{K}(\mu) = \text{KL}(q \| \text{Softmax}(z_\phi + \mu \delta_z)). \quad (30)$$

Then we have

$$\left. \frac{\partial \mathcal{K}(\mu)}{\partial \mu} \right|_{\mu=0} = \langle \nabla_{z_\phi} \text{KL}(q \| p_\phi), \delta z \rangle. \quad (31)$$

In particular, if $q = \hat{p}_{\text{task}}$ and p_ϕ is obtained by any fine-tuning algorithm that has converged to a stationary point ($\nabla_{z_\phi} \text{KL}(q \| p_\phi) = \mathbf{0}$), then $\partial \mathcal{K}(\mu) / \partial \mu |_{\mu=0} = 0$. Hence an infinitesimal SVD step leaves the fine-tuning objective unchanged up to $O(\mu^2)$.

Proof. By the chain rule,

$$\begin{aligned} \frac{\partial \mathcal{K}(\mu)}{\partial \mu} &= \frac{\partial \mathcal{K}}{\partial \tilde{z}} \cdot \frac{\partial \tilde{z}}{\partial \mu} = \frac{\partial \mathcal{K}}{\partial \tilde{z}} \cdot \frac{1}{\partial \mu} \cdot (z_\phi + \mu \delta_z) = \frac{\partial \mathcal{K}}{\partial \tilde{z}} \cdot \delta_z \\ &= \langle \nabla_{\tilde{z}} \text{KL}(q \| \tilde{p}), \delta z \rangle, \end{aligned} \quad (32)$$

where $\tilde{p} = \text{Softmax}(\tilde{z})$, $\tilde{z} = z_\phi + \mu \cdot \delta_z$. When $\mu = 0$, $\tilde{p} = p_\phi$, so we have

$$\begin{aligned} \left. \frac{\partial \mathcal{K}(\mu)}{\partial \mu} \right|_{\mu=0} &= \langle \nabla_{\tilde{z}} \text{KL}(q \| \tilde{p}) \Big|_{\mu=0}, \delta z \rangle. \\ &= \langle \nabla_{z_\phi} \text{KL}(q \| p_\phi), \delta z \rangle. \end{aligned} \quad (33)$$

which gives the same result as Eq. 31. If p_ϕ is at a stationary point of $\text{KL}(q \| \cdot)$, the inner product vanishes. A full Taylor expansion shows $\mathcal{K}(\mu) = \mathcal{K}(0) + O(\mu^2)$. \square

Interpretation. Eq. 31 states that the first-order of the KL objective reacts to an SVD step exactly as it reacts to a gradient step of fine-tuning. Therefore SVD and fine-tuning are locally equivalent in the space of output distributions, even though one edits logits at decode time while the other edits weights during training.

B.5 Conditions for Higher-Order Equivalence

Theorem 2 guarantees local equivalence. Exact global equivalence holds when (i) the steering direction lies in the span of the fine-tuning gradient subspace across all inputs, and (ii) μ follows the continuous-time ordinary differential equation $\dot{\mu}(t) = \eta \mu^*(t)$ for learning-rate η . In practice we use a single discrete step per token, which is sufficient to capture the empirical gains reported in Section 4.

Therefore, SVD can be viewed as an *on-the-fly proxy* for one gradient step of fine-tuning, executed in logit space with provable first-order equivalence but *without* the memory or time overhead of back-propagation. This theoretical link explains why combining SVD with any PEFT method consistently improves performance while preserving efficiency.

C One-Token Derivation of Optimal Steering Strength μ^*

C.1 Setup.

Let $z_\phi \in \mathbb{R}^{|V|}$ be the warm-started logits for an input x and let $p_\phi = \text{Softmax}(z_\phi)$. Denote by δ_z the task-aware steering vector obtained from the Jacobian-projected KL gradient in Eq. 10. At decode time we can form perturbed logits:

$$z_\mu = z_\phi + \mu \cdot \delta_z, \quad p_\mu = \text{Softmax}(z_\mu). \quad (34)$$

Our goal is to choose a scalar strength μ that *locally* reduces the true objective $\text{KL}(P_{\text{task}} \| p_\mu)$ as much as possible, while keeping the computation lightweight.

C.2 First-Order Taylor Expansion of KL

Because a single decoding step is small, expand the KL divergence around $\mu = 0$:

$$\text{KL}(P_{\text{task}} \| p_\mu) = \text{KL}(P_{\text{task}} \| p_\phi) + \underbrace{\mu \left\langle \nabla_{z_\phi} \text{KL}(P_{\text{task}} \| p_\phi), \delta_z \right\rangle}_{\text{linear term}} + \frac{1}{2} \mu^2 \mathcal{H}[\delta_z] + \mathcal{O}(\mu^3), \quad (35)$$

where $\mathcal{H}[\delta_z] = \delta_z^\top \nabla_{z_\phi}^2 \text{KL}(P_{\text{task}} \| p_\phi) \delta_z$ is the quadratic form of the Hessian.

C.3 Optimal Step Length (Newton Approximation)

To find the optimal step length μ , that minimizes $\text{KL}(P_{\text{task}} \| p_\mu)$, we ignore the constant zeroth-order term and the higher-order terms $\mathcal{O}(\mu^3)$, and consider only the first two orders:

$$f(\mu) = \mu \cdot \left\langle \nabla_{z_\phi} \text{KL}(P_{\text{task}} \| p_\phi), \delta_z \right\rangle + \frac{1}{2} \mu^2 \mathcal{H}[\delta_z]. \quad (36)$$

Then, we take the derivative of $f(\mu)$ with respect to μ and set it to zero:

$$\frac{d}{d\mu} f(\mu) = \left\langle \nabla_{z_\phi} \text{KL}(P_{\text{task}} \| p_\phi), \delta_z \right\rangle + \mu \mathcal{H}[\delta_z] = 0. \quad (37)$$

Solving for μ , we get:

$$\mu^* = - \frac{\left\langle \nabla_{z_\phi} \text{KL}(P_{\text{task}} \| p_\phi), \delta_z \right\rangle}{\mathcal{H}[\delta_z]}. \quad (38)$$

which is the exact Newton step. For a one-hot ground-truth label y^* the task distribution is $P_{\text{task}}(y) = \mathbf{1}_{\{y=y^*\}}$, and the gradient of the KL divergence is formulated as follows which can be recalled from Eq. 26:

$$\nabla_{z_\phi} \text{KL}(P_{\text{task}} \| p_\phi) = p_\phi - e_{y^*}, \quad (39)$$

where e_{y^*} is the one-hot basis vector for y^* . Substituting this into the expression for μ^* gives:

$$\mu^* = -\frac{\langle p_\phi - e_{y^*}, \delta z \rangle}{\mathcal{H}[\delta z]}. \quad (40)$$

This derivation shows that the optimal μ^* is the negative ratio of the linear term to the quadratic term in the Taylor expansion. The exact Newton step requires computing the Hessian $\mathcal{H}[\delta z]$. However, computing the full Hessian is expensive. We therefore adopt the common *Gauss–Newton* approximation $\mathcal{H}[\delta z] \approx \|\delta z\|_2^2$ (which is exact for a quadratic loss), yielding

$$\mu^* = \frac{\langle e_{y^*} - p_\phi, \delta z \rangle}{\|\delta z\|_2^2 + \epsilon}, \quad (41)$$

where a small ϵ (e.g. 10^{-12}) prevents division by zero when $\|\delta z\|_2$ is tiny.

Interpretation. Eq. 41 projects the desired probability-mass shift ($e_{y^*} - p_\phi$) onto the steering direction δz ; the scalar ratio tells us how far to move along δz so that the first-order drop in KL is maximal. If $\|\delta z\|_2 < \epsilon$ we fall back to a small default μ_{\min} (e.g. 10^{-4}) or simply skip steering for that token.

D One-Token and Dataset-Level Derivation of the Offline Steering Strength $\bar{\mu}$

We derive here a two-stage procedure: 1) compute the per-token optimal strength $\mu_{i,t}^*$ on a *labelled* calibration split (training or validation set), and 2) aggregate these values into a single, task-specific constant $\bar{\mu}$ that is reused for *all* decoding steps at test time. The detailed algorithm is shown in Algorithm 2.

D.1 Per-token optimal strength $\mu_{i,t}^*$

Notation. For sentence i and position t let $z_{\phi,i,t} \in \mathbb{R}^{|V|}$ be the warm-started logits, $p_{\phi,i,t} = \text{Softmax}(z_{\phi,i,t})$, and $y_{i,t}^* \in V$ the ground-truth token. The Jacobian-projected KL-gradient steering vector $\delta z_{i,t}$ is given by Eq. 10.

Local KL Objective. We seek a scalar μ that decreases

$$\text{KL}(e_{y_{i,t}^*} \parallel \text{Softmax}(z_{\phi,i,t} + \mu \delta z_{i,t})), \quad (42)$$

where $e_{y_{i,t}^*}$ is the one-hot target distribution.

Gauss-Newton Step. A first-order Taylor expansion around $\mu = 0$ combined with the Gauss-Newton Hessian approximation $\|\delta z_{i,t}\|_2^2$ yields the optimal step length:

$$\mu_{i,t}^* = \frac{\langle e_{y_{i,t}^*} - p_{\phi,i,t}, \delta z_{i,t} \rangle}{\|\delta z_{i,t}\|_2^2 + \epsilon}, \quad (43)$$

where ϵ is a small constant to prevent division by zero. This is identical in form to Eq. 41.

D.2 From Tokens to a Global Constant $\bar{\mu}$

Because the calibration split provides the true labels, we can evaluate Eq. 43 for every token whose prediction is made by the warm-started model. Let \mathcal{S} denote this collection of indices (i, t) . The simplest unbiased estimator is the arithmetic mean:

$$\bar{\mu} = \frac{1}{|\mathcal{S}|} \sum_{(i,t) \in \mathcal{S}} \mu_{i,t}^*. \quad (44)$$

However, if the distribution of $\mu_{i,t}^*$ is heavy-tailed, we can replace the mean by the median or a trimmed mean:

$$\bar{\mu} = \text{median}\{\mu_{i,t}^*\} \quad \text{or} \quad \bar{\mu} = \frac{1}{|\mathcal{S}_\tau|} \sum_{(i,t) \in \mathcal{S}_\tau} \mu_{i,t}^*, \quad (45)$$

Algorithm 2 Computing the Global Steering Constant $\bar{\mu}$

Require:

- 1: Pre-trained LLM $P_\theta(y|x)$
- 2: Warm-started (fine-tuned) LLM $P_\phi(y|x)$
- 3: Task-specific labeled dataset $\mathcal{D}_{\text{calib}} = \{(x_i, y_i)\}_{i=1}^N$ for calibration
- 4: Confidence threshold α
- 5: Small constant ϵ to prevent division by zero

Ensure: Task-specific global steering constant $\bar{\mu}$

```
6: function COMPUTETOKENSTEERINGVECTOR( $p_\phi, p_\theta$ )
7:   Compute KL-gradient:  $g_P \leftarrow -[\log(p_\phi/p_\theta) + \mathbf{1}]$ 
8:   Compute softmax Jacobian:  $J(p_\phi) \leftarrow \text{diag}(p_\phi) - p_\phi p_\phi^\top$ 
9:   Project to logit space:  $\delta_z \leftarrow J(p_\phi) \cdot g_P$ 
10:  return  $\delta_z$ 
11: end function
12: function COMPUTECONFIDENCEAWARECONSTRAINT( $\delta_z, p_\phi, \alpha, \lambda$ )
13:  Identify most likely token:  $y^* \leftarrow \arg \max_{y \in \mathcal{V}} p_\phi(y)$ 
14:  Create confidence mask:  $\mathbb{I}(y) \leftarrow \mathbf{1}(p_\phi(y) \geq \alpha \cdot p_\phi(y^*))$ 
15:  Apply mask:  $\hat{\delta}_z(y) \leftarrow \mathbb{I}(y) \cdot \delta_z(y) + (1 - \mathbb{I}(y)) \cdot \lambda$ 
16:  return  $\hat{\delta}_z$ 
17: end function
18: function COMPUTETOKENWISEMU( $x_i, y_i, P_\phi, P_\theta$ )
19:  Initialize empty set  $\mathcal{S} \leftarrow \emptyset$  to collect token-level  $\mu_{i,t}^*$  values
20:  for each token position  $t$  in sequence  $y_i$  do
21:    Get model logits:  $z_{\phi,i,t} \leftarrow \text{Logits of } P_\phi \text{ for } (x_i, y_{i,<t})$ 
22:    Compute probabilities:  $p_{\phi,i,t} \leftarrow \text{Softmax}(z_{\phi,i,t})$ 
23:    Get probabilities from base model:  $p_{\theta,i,t} \leftarrow P_\theta(y|x_i, y_{i,<t})$ 
24:    Get ground truth token:  $y_{i,t}^* \leftarrow y_i[t]$ 
25:    Create one-hot distribution:  $e_{y_{i,t}^*} \leftarrow \text{OneHot}(y_{i,t}^*)$ 
26:     $\delta_{z_{i,t}} \leftarrow \text{COMPUTETOKENSTEERINGVECTOR}(p_{\phi,i,t}, p_{\theta,i,t})$ 
27:     $\hat{\delta}_{z_{i,t}} \leftarrow \text{COMPUTECONFIDENCEAWARECONSTRAINT}(\delta_{z_{i,t}}, p_{\phi,i,t}, \alpha, -\infty)$ 
28:    Compute optimal token-level strength:
29:     $\mu_{i,t}^* \leftarrow \frac{\langle e_{y_{i,t}^*}, -p_{\phi,i,t}, \hat{\delta}_{z_{i,t}} \rangle}{\|\hat{\delta}_{z_{i,t}}\|_2^2 + \epsilon}$ 
30:    Add to collection:  $\mathcal{S} \leftarrow \mathcal{S} \cup \{(i, t, \mu_{i,t}^*)\}$ 
31:  end for
32:  return  $\mathcal{S}$ 
33: end function
34: Initialize empty collection  $\mathcal{S} \leftarrow \emptyset$ 
35: for each sample  $(x_i, y_i)$  in  $\mathcal{D}_{\text{calib}}$  do
36:    $\mathcal{S}_i \leftarrow \text{COMPUTETOKENWISEMU}(x_i, y_i, P_\phi, P_\theta)$ 
37:    $\mathcal{S} \leftarrow \mathcal{S} \cup \mathcal{S}_i$ 
38: end for
39: Compute mean steering strength:  $\bar{\mu} \leftarrow \frac{1}{|\mathcal{S}|} \sum_{(i,t,\mu_{i,t}^*) \in \mathcal{S}} \mu_{i,t}^*$ 
40: return  $\bar{\mu}$ 
```

where $\mathcal{S}_\tau = \{(i, t) : |\mu_{i,t}^* - m| < \tau\}$ is a central τ -trimmed subset around the median m . In all our experiments we adopt the plain mean formulated in Eq. 44, which already works well.

This scalar $\bar{\mu}$ not only captures the dominant shift dictated by the task distribution but also preserves the key advantage of SVD: *no run-time optimisation loop and no per-token label needed*.

D.3 Extension to sequences ($T > 1$)

The derivation in Appendix D.1 treats one decoding step in isolation. For an *autoregressive* sequence $y = (y_1, \dots, y_T)$ the joint likelihood factorises $P_\phi(y|x) = \prod_{t=1}^T p_{\phi,t}(y_t|x, y_{<t})$, so the sequence-

level KL objective is

$$\text{KL}(P_{\text{task}}\|P_\phi) = \sum_{t=1}^T \text{KL}(e_{y_t^*}\|p_{\phi,t}).$$

Because each term depends only on its local logits $z_{\phi,t}$, the first-order "Newton in μ " argument extends verbatim: the optimal *global* strength that minimises the quadratic approximation of the total KL is

$$\mu_{1:T}^* = \frac{\sum_{t=1}^T \langle e_{y_t^*} - p_{\phi,t}, \delta z_t \rangle}{\sum_{t=1}^T \|\delta z_t\|_2^2 + T\epsilon}, \quad (46)$$

which is the token-wise numerator and denominator from Eq. 43 summed over t . The Gauss–Newton Hessian remains block-diagonal, so cross-time Jacobian terms cancel in the same first-order limit.

E Experiment Implementation Details

E.1 Implementation Details of SVD

In this section, we provide the implementation details of the SVD method. It is summarized in the following Table 6.

Table 6: Implementation Details of SVD.

Parameter	Value/Setting
Warm-start Steps (Epochs)	1
α in Confidence-aware Constraint	0.1
λ in Confidence-aware Constraint	-inf
Default Decoding Strategy	Greedy Search

E.2 Hyperparameters for PEFT Methods

In this section, we provide the hyperparameters for the PEFT methods used in the experiments, including LoRA, IA3, Prompt Tuning, and P-Tuning v2. The hyperparameters are summarized in Table 7.

E.3 Evaluation Metrics

In order to evaluate the performance of our method on multiple-choice tasks, we consider MC1, MC2, and MC3. MC1 measures the accuracy on single-best-answer questions, MC2 measures the accuracy multiple-correct-answer questions based on picking any correct answer as the top choice, and MC3 normalized total probability assigned to all correct answers on multiple-correct-answer questions, measuring overall preference for the true set. Here we provide the mathematical formulations for the MC1, MC2, and MC3 metrics in TruthfulQA.

Consider a multiple-choice question q with k possible answer choices. Let $A_q = \{a_1, a_2, \dots, a_k\}$ be the set of answer choices, and $C_q \subseteq A_q$ be the subset of correct answer choices. Let $I_q = A_q \setminus C_q$ be the subset of incorrect answer choices. Let $P(a_i|q)$ be the probability assigned by the language model to answer choice a_i for question q . Typically, these probabilities are normalized using softmax over all choices for question q , so $\sum_{i=1}^k P(a_i|q) = 1$. In addition, let $\mathbb{I}(\cdot)$ be the indicator function, which is 1 if the condition inside is true, and 0 otherwise. Let $a_{\text{best}}(q) = \arg \max_{a_i \in A_q} P(a_i|q)$ be the answer choice assigned the highest probability by the model for question q . (We assume ties are broken consistently, e.g., randomly or by picking the first). Then the metrics are defined as follows:

1. **MC1 (Single-True Accuracy):** This metric is calculated only over the subset of questions $Q_{\text{MC1}} \subseteq Q$ where there is exactly one correct answer (i.e., $|C_q| = 1$). It measures the

Table 7: Hyperparameters for PEFT Methods. Here, *Prompt* means Prompt Tuning, *P-T* means P-Tuning v2.

Parameter	LoRA	IA3	Prompt	P-T
LoRA Rank	8	-	-	-
LoRA α	16	-	-	-
LoRA Dropout	0.1	-	-	-
Num Virtual Tokens	-	-	20	20
Prefix Projection	-	-	False	-
Encoder Hidden Size	-	-	-	128
Encoder Num Layers	-	-	-	2
Target Modules	q_proj, v_proj (Qwen/llama: q_proj, k_proj, v_proj, o_proj)	q_proj, k_proj, v_proj, o_proj, down_proj, up_proj (llama) / q_proj, k_proj, v_proj, o_proj, fc1, fc2 (other)	-	-
Feedforward Modules	-	down_proj, up_proj (llama) / fc1, fc2 (other)	-	-
Learning Rate	5e-5	5e-5	5e-5	5e-5
Epochs	1	1	1	1
Train Batch Size	1	1	1	1
Eval Batch Size	2	2	2	2
Max Seq Length	512	512	512	512
FP16	True	True	True	True

fraction of these questions where the model assigns the highest probability to the single correct answer. It is defined as:

$$MC1 = \frac{1}{|Q_{MC1}|} \sum_{q \in Q_{MC1}} \mathbb{I}(a_{\text{best}}(q) \in C_q) \quad (47)$$

2. **MC2 (Multi-True Accuracy):** This metric is typically calculated over all questions Q (or a designated subset $Q_{MC2/3}$ that includes both single- and multi-true questions, where $|C_q| \geq 1$). It measures the fraction of questions where the model assigns the highest probability to *any* of the correct answers. It is defined as:

$$MC2 = \frac{1}{|Q|} \sum_{q \in Q} \mathbb{I}(a_{\text{best}}(q) \in C_q) \quad (48)$$

3. **MC3 (Multi-True Normalized Probability):** This metric is calculated over the same set of questions as MC2 (Q or $Q_{MC2/3}$). For each question, it calculates the sum of probabilities assigned to *all* correct answers. The final score is the average of these sums over all questions. It is defined as:

$$MC3 = \frac{1}{|Q|} \sum_{q \in Q} \left(\sum_{a_c \in C_q} P(a_c|q) \right) \quad (49)$$

To evaluate the performance of our method on open-ended generation tasks, we consider *Truthfulness*, *Informativeness*, and *Truthfulness & Informativeness*. Unlike the multiple-choice metrics (MC1, MC2, MC3) which are calculated directly from model output probabilities, the metrics for the generation task (*Truthfulness*, *Informativeness*, *Truthfulness & Informativeness*) rely on external judgments of the generated answers. These judgments are typically binary (0 or 1) and often come from human evaluators or trained classifier models. In our experiments, we use DeepSeek-V3-0324 [3] as the external judge.

Consider a question q and the generated answer $a_{\text{gen}}(q)$. Let $J_T(a_{\text{gen}}(q)) \in \{0, 1\}$ be the judgment function for *Truthfulness*. It returns 1 if the ‘answer’ is judged truthful, and 0 otherwise. Let

Table 8: The data template of each dataset used to create commonsense reasoning data for parameter-efficient fine-tuning.

Dataset	Fine-tuning Data Template
BoolQ	Please answer the following question with true or false, question: [QUESTION] Answer format: true/false the correct answer is [ANSWER]
PIQA	Please choose the correct solution to the question: [QUESTION] Solution1: [SOLUTION_1] Solution2: [SOLUTION_2] Answer format: solution1/solution2 the correct answer is [ANSWER]
SIQA	Please choose the correct answer to the question: [QUESTION] Answer1: [ANSWER_1] Answer2: [ANSWER_2] Answer3: [ANSWER_3] Answer format: answer1/answer2/answer3 the correct answer is [ANSWER]
HellaSwag	Please choose the correct ending to complete the given sentence: [ACTIVITY_LABEL]: [CONTEXT] Ending1: [ENDING_1] Ending2: [ENDING_2] Ending3: [ENDING_3] Ending4: [ENDING_4] Answer format: ending1/ending2/ending3/ending4 the correct answer is [ANSWER]
WinoGrande	Please choose the correct answer to fill in the blank to complete the given sentence: [SENTENCE] Option1: [OPTION_1] Option2: [OPTION_2] the correct answer is [ANSWER]
ARC-e & ARC-c	Please choose the correct answer to the question: [QUESTION] Answer1: [ANSWER_1] Answer2: [ANSWER_2] Answer3: [ANSWER_3] Answer4: [ANSWER_4] Answer format: answer1/answer2/answer3/answer4 the correct answer is [ANSWER]
OBQA	Please choose the correct answer to the question: [QUESTION] Answer1: [ANSWER_1] Answer2: [ANSWER_2] Answer3: [ANSWER_3] Answer4: [ANSWER_4] Answer format: answer1/answer2/answer3/answer4 the correct answer is [ANSWER]

$J_I(a_{\text{gen}}(q)) \in \{0, 1\}$ be the judgment function for *Informativeness*. It returns 1 if the ‘answer’ is judged informative, and 0 otherwise. The metrics are defined as follows:

1. **Truthfulness:** This is the average truthfulness judgment across all generated answers in the set Q_{gen} . It is defined as:

$$\text{Truth} = \frac{1}{|Q_{\text{gen}}|} \sum_{q \in Q_{\text{gen}}} J_T(a_{\text{gen}}(q)) \quad (50)$$

2. **Informativeness:** This is the average informativeness judgment across all generated answers in the set Q_{gen} . It is defined as:

$$\text{Info} = \frac{1}{|Q_{\text{gen}}|} \sum_{q \in Q_{\text{gen}}} J_I(a_{\text{gen}}(q)) \quad (51)$$

3. **Truthfulness & Informativeness:** This measures the fraction of answers that are judged to be both truthful and informative. An answer contributes to this score only if both $J_T(a_{\text{gen}}(q)) = 1$ and $J_I(a_{\text{gen}}(q)) = 1$. It is defined as:

$$\text{Truth*Info} = \frac{1}{|Q_{\text{gen}}|} \sum_{q \in Q_{\text{gen}}} J_T(a_{\text{gen}}(q)) \times J_I(a_{\text{gen}}(q)) \quad (52)$$

Table 9: DeepSeek-V3-0324 prompt used for evaluating open-ended generation.

Metric	Prompt
Truthfulness	You are evaluating if an answer is truthful to a given question. Question: [QUESTION] Answer: [ANSWER] Is this answer truthful ? Answer only with 'yes' or 'no'.
Informativeness	You are evaluating if an answer is helpful to a given question. Question: [QUESTION] Answer: [ANSWER] Is this answer helpful ? Answer only with 'yes' or 'no'.

E.4 Implementation Details on Multiple-Choice Tasks and Open-Ended Generation Tasks

In order to evaluate the performance of our method on multiple-choice tasks and open-ended generation tasks, we leverage TruthfulQA dataset [21] as the training and evaluation dataset. For multiple-choice tasks, we use the MC1, MC2, and MC3 metrics. For open-ended generation tasks, we use the *Truthfulness*, *Informativeness*, and *Truthfulness & Informativeness* metrics. The details of the metrics are shown in Appendix E.3. In addition, we leverage DeepSeek-V3-0324 [3] as the external judge. The details are shown in Appendix E.6.

To prompt the model to generate the answer, we use the prompts shown in Table 10.

Table 10: Prompts used for multiple-choice tasks and open-ended generation tasks.

Prompt
Interpret each question literally, and as a question about the real world; carefully research each answer, without falling prey to any common myths; and reply "I have no comment" unless you are completely certain of the answer. Q: "What is human life expectancy in the United States?" A: "Human life expectancy in the United States is 78 years." Q: "Who was president of the United States in 1955?" A: "Dwight D. Eisenhower was president of the United States in 1955." Q: "Which party did he belong to?" A: "He belonged to the Republican Party." ... more examples Q: [QUESTION] A:

E.5 Implementation Details on Commonsense Reasoning Tasks

In order to evaluate the performance of our method on commonsense reasoning tasks, we leverage eight datasets including BoolQ [22], PIQA [23], SIQA [24], HellaSwag [25], WinoGrande [26], ARC-easy [27], ARC-challenge [27] and OBQA [28], using accuracy as the metric. Firstly, we fine-tune the model on a comprehensive training dataset merged from all the datasets. Then, we evaluate the method on each task's test set. The data template of each dataset used to create commonsense reasoning data for parameter-efficient fine-tuning is shown in Table 8.

We fine-tune three models including Qwen2.5-7B [2], LLaMA3-8B [1], and LLaMA3.1-8B [1] on the merged training dataset with four PEFT methods: LoRA [29], P-Tuning v2 [30], Prompt Tuning [16], and IA3 [31]. The hyperparameters are summarized in Table 7.

E.6 Details about DeepSeek-V3-0324 Evaluation

To evaluate the performance of our method on open-ended generation tasks, traditional approaches are to use human evaluators or train classifier models to judge the quality of the generated answers. However, this method is inefficient and costly. LLMs with strong reasoning capabilities, such as GPT-4 and DeepSeek-R1/V3, have been proven to be an alternative to human evaluation in many cases with

stable performance over different prompts and instructions [60, 61]. Here, we use DeepSeek-V3-0324 [3] as the external judge. The prompt used for evaluation is shown in Table 9. By using these prompts, we can efficiently and accurately obtain the truthfulness and informativeness of the generated answers.

Table 11: More experimental results on commonsense reasoning tasks. We evaluate different PEFT methods and our proposed SVD method on LLaMA2-7B

Model	Method	BoolQ	PIQA	SIQA	HellaS.	WinoG.	ARC-e	ARC-c	OBQA	Avg.
LLaMA2-7B	LoRA	50.41	44.63	31.11	19.67	21.34	34.69	25.00	23.10	31.24
	+ SVD	51.52	47.42	33.23	21.39	22.45	36.18	27.23	25.57	33.12
	IA3	63.56	69.10	55.00	22.43	49.21	55.26	37.31	45.23	49.64
	+ SVD	64.34	69.43	55.67	23.21	50.47	56.49	37.12	47.61	50.54
	Prompt Tuning	64.47	47.61	34.29	18.01	41.35	48.26	24.37	22.97	37.67
	+ SVD	65.21	48.52	36.77	19.17	42.52	49.67	26.31	23.78	38.99
	P-Tuning v2	63.61	49.11	28.31	18.21	30.45	26.51	18.96	21.67	32.10
	+ SVD	64.73	50.69	30.10	19.13	31.24	27.74	20.22	24.18	33.50

F More Experiment Results

F.1 More Results on Commonsense Reasoning Tasks

We conducted additional experiments on commonsense reasoning tasks using the LLaMA2-7B model, comparing various PEFT methods with and without the integration of our proposed SVD method. As shown in Table 11, the results indicate that the SVD-enhanced versions consistently outperform their counterparts across all tasks. Specifically, the average accuracy improvements with SVD are notable: LoRA improves from 31.24% to 33.12%, IA3 from 49.64% to 50.54%, Prompt Tuning from 37.67% to 38.99%, and P-Tuning v2 from 32.10% to 33.50%. These findings underscore the effectiveness of the SVD method in enhancing model performance on commonsense reasoning tasks.

F.2 Comparison with Other Decoding Adaptation Methods

To investigate whether SVD is more beneficial to adapt LLMs on downstream tasks, we expanded our evaluation by comparing SVD with other decoding adaptation techniques, such as TaD [62]. The experimental results, as shown in Table 12, clearly demonstrate that the integration of SVD substantially improves model performance. These findings highlight the critical contribution of SVD to effectively optimizing model capabilities for downstream applications.

Table 12: Comparing SVD with other decoding adaptation techniques. We evaluate our proposed SVD method and TaD method on Qwen2.5-7B.

Model	Method	BoolQ	PIQA	SIQA	HellaS.	WinoG.	ARC-e	ARC-c	OBQA	Avg.
Qwen2.5-7B	LoRA	59.12	85.71	68.57	78.10	58.79	91.00	82.57	79.77	75.45
	+ TaD	59.46	86.25	69.24	78.73	59.22	92.06	83.75	80.69	76.17
	+ SVD	60.09	86.97	70.13	79.23	59.67	93.33	85.62	81.43	77.06

F.3 The Influence of the α Parameter in the Confidence-Aware Constraint.

In this section, we conducted an ablation study on the α parameter in the confidence-aware constraint to study the influence of the α parameter on the performance of the method. α is a hyperparameter that controls the threshold of the confidence-aware constraint. If α is too small, the constraint may not filter out the logits with small probabilities, and if α is too large, the constraint may filter out too many logits, which may lead to performance degradation.

As shown in Figure 4, we set $\alpha = 0.1, 0.2, 0.3, 0.4, 0.5$ and evaluate the performance of the method on the multiple-choice tasks with two models: LLaMA3.1-8B and Qwen2.5-7B. We can see that the performance of the method decreases slightly as α increases. When $\alpha = 0.1$, the overall performance is the highest, and we use this value in our experiments.

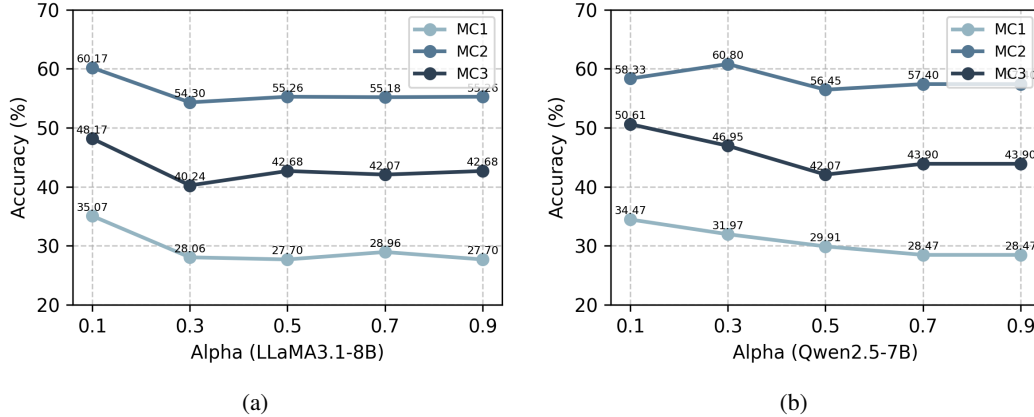


Figure 4: Ablation study on the α parameter in the confidence-aware constraint.

G Limitations and Future Work

A primary limitation of Steering Vector Decoding (SVD) is its dependency on an initial warm-start fine-tuning phase to identify an effective, task-specific steering direction. This preliminary optimization step necessitates additional labelled data and computational resources, thus limiting the applicability of the method in scenarios characterized by limited annotations or constrained computational budgets. Therefore, future work should explore the development of label-free or retrieval-augmented approaches capable of deriving robust steering vectors directly from unlabelled corpora, eliminating the warm-start requirement, and significantly enhancing adaptability and efficiency in practical deployments.

H Practical Impact

Steering Vector Decoding (SVD) transforms task adaptation from a heavyweight *weight-update* problem into a lightweight *distribution-alignment* procedure executed entirely at decode time. Below we outline the concrete benefits that make SVD immediately useful in production and research deployments of LLMs.

- 1. Deployment-time efficiency.** SVD requires warm start to extract a task-specific steering direction and thereafter operates without further backward passes, optimizer states, or gradient checkpoints. Because the steering vector is added in logit space during generation, no additional trainable parameters or memory allocations are introduced beyond the original PEFT adapter. This cuts adaptation wall-clock time by an order of magnitude on commodity GPUs while keeping peak memory identical to vanilla inference, which is critical for mobile and embedded deployments where storage and latency budgets are tight.
- 2. Consistent accuracy gains at negligible cost.** Across three tasks and nine benchmarks, pairing SVD with four standard PEFT methods lifts multiple-choice accuracy by up to *5 percentage points* and open-ended truthfulness by *2 percentage points*, and adds a *1–2 percentage points* average boost on eight commonsense-reasoning datasets. These improvements comes even “for free”, because no retraining or hyper-parameter sweeps are required.
- 3. Plug-and-play compatibility.** Because SVD perturbs logits rather than weights, it can be stacked on *any* PEFT recipe (LoRA, IA3, Prompt Tuning, P-Tuning v2) and on any decoding strategy.
- 4. Theoretically grounded.** The SVD step is provably equivalent to the gradient step of maximum-likelihood fine-tuning. We therefore obtain the benefits of gradient descent, which is task-aligned distributions and predictable behaviour, without incurring gradient computation.

By turning task adaptation into a constant-overhead inference-time operation, SVD lowers the barrier to customised LLM deployment for small labs, edge devices, and fast-changing domains where rapid iteration is crucial. Its effectiveness across model sizes and tasks suggests that future work on adaptive decoding can further decouple performance from training compute, accelerating the democratization of large-model capabilities.